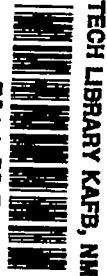# NATIONAL ADVISORY COMMITTEE
FOR AERONAUTICS

TECHNICAL MEMORANDUM 1392

ON THE BUCKLING OF BARS AND PLATES IN THE PLASTIC RANGE

Part II

By J. P. Benthem

Translation of "Over het knikvraagstuk in het plastische gebied bij
staven en platen. (Deel II)." Nationaal Luchtvaartlaboratorium,
Amsterdam, Rapport S. 423, Jan. 1954.

NACA

Washington
March 1956

1K

NATIONAL ADVISORY COMMITTEE FOR AERONAUT

TECHNICAL MEMORANDUM 1392

ON THE BUCKLING OF BARS AND PLATES IN THE PLASTIC RANGE[*]

Part II

By J. P. Benthem

NOTATIONS

a	length of rectangular plate
b	width of rectangular plate
h	thickness of rectangular plate
x	coordinate along plate length
y	coordinate along plate width
σ_x, σ_y	normal stress components σ_x and σ_y generally counted positive when compressive stresses
τ	shear stress component
ϵ_x, ϵ_y	normal strain components ϵ_x and ϵ_y generally counted positive for compressive strains
γ	shearing strain component
$\bar{\sigma}$	critical state of stress
$\bar{\epsilon}$	critical state of deformation
$\bar{\sigma}_e$	critical stressed state computed by elasticity theory
$\bar{\epsilon}_e$	critical state of deformation computed by elasticity theory
$\bar{\sigma}_x$	critical stress σ_x of a rectangular plate under uniform load in the length direction
$\bar{\epsilon}_x$	corresponding strain ϵ_x

---

[*]"Over het knikvraagstuk in het plastische gebied bij staven en platen. (Deel II)." Nationaal Luchtvaartlaboratorium, Amsterdam, Rapport S. 423, Jan. 1954.

$\bar{\sigma}_{x,e}, \bar{\epsilon}_{x,e}$ the same, computed by elasticity theory

$\bar{\tau}$ critical shear stress τ of rectangular plate loaded in shear

$\bar{\gamma}$ corresponding shearing strain γ

$\bar{\tau}_e, \bar{\gamma}_e$ the same, computed by elasticity theory

k   so-called buckling factor — a nondimensional factor appearing in one formula in the form (see section 2.2)

$$\bar{\sigma} = \frac{k\pi^2 E b^2}{12(1 - \nu^2)h}$$

k_e buckling factor computed by elasticity theory

$\eta = \sigma/\bar{\sigma}_e = k/k_e$

E   Young's modulus

E_t tangent modulus, that is, $d\sigma_x/d\epsilon_x$ of the stress-strain diagram of the tension and compression test

E_{sec} secant modulus, that is, σ_x/ϵ_x of the stress-strain diagram from the tension and compression test

E_r reduced modulus according to (3.5)

α E/E_r

G   shear modulus

ν Poisson's ratio, that is, $-\epsilon_x/\epsilon_y$ of the bar stressed in tension or compression along x into the elastic range

ν' the quotient of $-\epsilon_y/\epsilon_x$ of the bar stressed in tension or compression along x into the plastic range

2. INTRODUCTION

Part I of this report (ref. 1) dealt with the buckling of plates in the elastic range on the basis of two different kinds of plasticity

theories, the so-called deformation theory and the so-called incremental theory.

It is now generally accepted that, from the physical point of view, incremental theories give a rather good picture of the plastic deformation (compare refs. 2, 3, and 4) and that deformation theories certainly cannot be correct (refs. 2 and 3). However, it still seems that the results for the critical buckling loads of plates, loaded in the plastic range, are substantially higher when computed by incremental theory than indicated by the test.

The experimental values are correct in the neighborhood of the results by deformation theory, although quite often the "excellent agreement" spoken of does not exist.

The failure of incremental theories for defining the critical buckling load in the plastic range is frequently regarded as proof of the inaccuracy of incremental theories themselves, but that is entirely unjust. As Prager so rightly remarked (in ref. 5): "To this writer (Prager) the idea of testing a stress-strain law by buckling experiments seems utterly fantastic; nobody would dream of determining, say, Young's modulus by a buckling test in the elastic range rather than a simple tension test. Direct experiments speak in favor of incremental theories, and there are strong theoretical objections against deformation theories."

Batdorf and Budiansky (ref. 6, see also refs. 3 and 1) developed a theory which, for certain load increases, gives results according to a deformation theory. Their theory has less physical faults than deformation theory itself, but some direct checks on this theory come out badly.

Besseling (ref. 1) sums up some of the possible causes of the failure of incremental theories and also cites the report by Onat and Drucker (ref. 7). The last-named report shows, on a special load case, how small initial eccentricities exert a very strong reducing effect on a critical buckling load computed by incremental theories, as shall be explained in section 3.5. That section deals also with a special investigation that indicates how the stress-strain relations by both theories vary when, at a constant compressive load above the elastic limit, a shear stress, increasing from zero, is applied.

In practice, it is hardly possible, of course, to include initial eccentricities in the calculations; they should also be exactly known. The fact that then all points of a plate have different stress-strain relations (which in the special load case used by Onat and Drucker was not the case) raises well-nigh prohibitive mathematical difficulties.

The question of whether the calculation by deformation theory is the right way forms the subject of the present report. Yet, before applying

deformation theories to buckling problems of plates — and this is accomplished before passing to incremental theories — some simple calculating methods are given which, compared with the experiment, did not give such bad results.

2. STATEMENT OF RESULTS

2.1 INTRODUCTION

On a rectangular plate, loaded in its plane by a uniform stressed state, the components of which are defined by a constant factor, the critical state of stress indicated by $\bar{\sigma}$ is defined by length a, width b, plate thickness h, by the clamping at the edges and by the material properties. Variation of the linear plate dimensions in the same ratio leaves the stress or strain components in the critical state unchanged.

By "load case" is meant a case in which a rectangular plate of specific material and with specified attachments at the edges, changes to a uniform state of stress before reaching the critical state, and whereby the stress components have a certain fixed relationship.[1] To illustrate: a rectangular plate of a certain material, clamped at the edges in uniform state of shear stress, is a load case. Another one is the rectangular plate of a certain material with hinge-supported edges in uniform state of normal stress (with respect to a pair of sides).

2.2 Variation of Length-Width Ratio

The critical stressed state $\bar{\sigma}$ for a specific load case is, as far as the plate dimensions are concerned, simply dependent on two independent variables, such as the length-width ratio a/b or the width-thickness ratio b/h.

$$\bar{\sigma} = f\left(\frac{a}{b}, \frac{b}{h}\right) \tag{2.1}$$

Figure 2.1 represents a diagram for constant width-thickness ratio, the critical load plotted against the length-width ratio.

---

[1]Only such load cases are treated. Plates other than rectangular are excluded, so also plates whose stressed state before reaching the critical stressed state is not uniform, although defined by a constant factor, such as the web of a beam under moment load or shear, for example.

The different branches of the curve correspond to different numbers (m) of half-waves. The number of half-waves computed by different plasticity theories or elasticity theory need not be identical for a given load case a/b.

By (3.1) it follows that the critical stress $\bar{\sigma}$ for a given load case in the elastic range can be written

$$\bar{\sigma} = \frac{D}{h} g(a,b) = \frac{D}{h} \frac{1}{b^2} j(a,b) \qquad (2.2)$$

where g and j are functions of the rectangular sides a and b. Examination of the dimensions of $\bar{\sigma}$, D, and h indicates that function j is dimensionless. Thence by (3.2)

$$\bar{\sigma} = \frac{\pi^2 k D}{h b^2} = \frac{k \pi^2 E h^2}{12(1 - \nu^2) b^2} \qquad (2.3)$$

with k a function of the length-width ratio a/b. The formula (2.3) is, naturally, in agreement with the form of (2.1).

Formula

$$\bar{\sigma} = \frac{\pi^2 k' D}{h a^2} \quad \text{with} \quad k' = \left(\frac{a}{b}\right)^2 k \qquad (2.4)$$

is, of course, valid too.

The square of the side b loaded in compression is chosen in the denominator of formula (2.3) for the plate compressed in one direction, solely because otherwise the limit transition to a → ∞ becomes difficult.

The coefficient k in (2.3) is called the buckling factor.

The critical stress state in the plastic range is indicated by a different function of the ratio b/h than given in (2.3), though the form of (2.3) is also used in this range, but then the buckling factor k is no longer a function of a/b but of b/h too.

2.3. VARIATION OF THE WIDTH-THICKNESS RATIO

2.3.1. Kollbrunner Method

When setting up the length-width ratio, the width-thickness ratio remains merely as variable. The length-width ratio of an infinitely long plate can equally be considered as fixed when the critical load at approaching ∞ plate length does not approach zero.

Figure 2.2, taken from Kollbrunner's report (ref. 11), represents the critical load of an infinitely long plate supported by hinges on the long edges and under lengthwise compression plotted against what Kollbrunner calls the slenderness

$$\lambda = \frac{b}{h}\sqrt{12(1 - \nu^2)}$$

2.3.2. U. S. Methods

2.3.2.1.- When the length-width ratio of a plate is fixed (for the plate of infinite length this means, if the condition cited in section 2.3 is complied with), the NACA does not select the width-thickness ratio b/h as independent variable, but the critical state of stress or critical state of strain, as computed by elasticity theory. The thus computed states are, for a certain load case, with fixed length-width ratio, naturally simple functions of the b/h ratio, and therefore can supersede the last named ratio as variable.

In figure 2.3 the (actual) critical state of stress (vertical) is shown plotted against the critical state of strain computed by elasticity theory (horizontal). When, as in figure 2.3, the critical strain condition computed by elasticity theory is plotted horizontal, the NACA usually employs the term "strain" or "shear." This simple indication is often too indefinite, since on the vertical the term "stress" or "shear stress" is used also (i.e., the actual critical stress or shear stress). Some writers, like Schuette and MacDonald (ref. 10), even call the curve in a diagram with such indications the "plate compressive curve," by which the impression is gained as if the diagram gave the relationship between stress and strain (or crushing of plate divided by height = mean strain) of a plate during a loading process.

By chance the curve in a diagram of the discussed calculating method by Gerard (section 3.2) was exactly identical with the stress-strain curve of the material. The true significance of the diagram is, however, an entirely different one; it gives the critical state of stress in terms of the width-thickness ratio. Some writers who use other computing methods

than Gerard's frequently plot, besides their computed curve, or besides
test points, the actual stress-strain curve of the material. This has
the advantage of making the value of the critical strain available while
reading off a critical stress value.

2.3.2.2.- From a diagram as discussed in section 2.3.2.1 where a
critical stress $\bar{\sigma}$ is plotted against $\bar{\sigma}_e$ computed by elasticity theory,
another one can be constructed in which

$$\eta = \frac{\bar{\sigma}}{\bar{\sigma}_e} \quad \text{against} \quad \bar{\sigma}$$

This form of diagram is also much used by the NACA. $\bar{\sigma}$ (horizontal)
against $\bar{\sigma}/\bar{\sigma}_e$ (vertical).

In this manner figure 2.4 was derived from figure 2.3. Point A in
figure 2.3 has the coordinates: 0.008 and 60,000 lb/inch^2. Young's
modulus is $E = 10.7 \times 10^6$ lb/inch^2. The corresponding point A in fig-
ure 2.4 has then 60,000 lb/inch^2 as abscissa and
$\eta = 60,000/0.008 \times 10.7 \times 10^6 = 0.7$ as ordinate. The factor η can be
expressed by

$$\eta = \frac{k}{k_e}$$

with k the buckling factor and k_e the buckling factor by elasticity
theory.

The factor η is always the factor with which the critical load
computed by elasticity theory must be multiplied in order to obtain the
actual critical load. Formulas applicable in the elastic range cannot
only be generalized by giving the buckling factor k another value than
by elasticity theory, but also by retaining the value of k by elastic-
ity theory when adding the factor η to the particular formula. The
factor ηE appearing then in such a formula is called the buckling
modulus, as by Kollbrunner in reference 8.[2]

2.3.2.3.- Besseling (in ref. 1) uses a diagram in still another
form; not $\eta = \bar{\sigma}/\bar{\sigma}_e$ plotted against $\bar{\sigma}$, but buckling factor $k = \eta k_e$
plotted against critical strain $\bar{\epsilon}$, which, however, is associated with
the critical stress $\bar{\sigma}$ in very simple manner. For the plate compressed
in one direction it naturally gives $\bar{\epsilon} = \bar{\sigma}/E_{sec}$. Figure 3.4 represents
such a diagram.

_____
[2]The same writer calls the tangent modulus "variable elasticity
modulus" in reference 8.

3. THEORIES OF PLASTICITY USED TO DEFINE THE CRITICAL

BUCKLING LOAD OF PLATES

3.1. INTRODUCTION — SHANLEY EFFECT

If a plate, loaded in its plane only, and hence being initially in
the state of stress of a membrane, is subjected to a deflection perpendi-
cular to its plane, bending and torsion stresses arise, and therefore
the stress or the criterion for further plastic deformation (generally
the distortion energy) over a section of the plate thickness decreases.
If the plate in its uniform state of stress was already loaded as far as
in the plastic range, the appearance of a deflection perpendicular to the
plane of the plate makes the corresponding deformation partly plastic and
partly elastic, which complicates the calculations.

Shanley (ref. 12), however, pointed out that the first appearance of
a deflection in consequence of reaching the critical buckling load is
still accompanied by further simultaneous deformation in the plane of
the plate, so that progressive plastic deformation takes place everywhere.
In fact, there is no buckling process at all in the ordinary sense of the
word (i.e., a process that takes place while the outside loads remain
constant).

Shanley applied this principle to the straight bar under column load,
and established that the start of the buckling process can be identified
by replacing Young's modulus E in the formulas for the buckling load in
the elastic range by the tangent modulus E_t. As a rule, any further
deflection is accompanied by a slight load increase only, so that the
load at which deflection can start may be defined as "buckling load."
This had been done in the past, obviously unconsciously, but later on
E_r (a reduced modulus) lying between E and E_t was used, as the
buckling process was considered a constant load process in which, in
fact, unloading takes place in a part of the bar.

This calculation with "Shanley effect" is found also in the treat-
ment of plates. Nowadays it is assumed that the calculation can be car-
ried out as if the Shanley effect over the whole plate did occur. In
other words, a critical buckling load in the plastic range is calculated
solely by stress-strain relations applicable to progressive plastic defor-
mation. But the result will not be such, even by approximation, that E
can be replaced by E_t in the elastic formulas, in order to get the
desired result as is the case in the buckling of bars.

3.2. FIRST ATTEMPTS

The differential equation of a buckled isotropic plate loaded in its plane has, in the elastic range, the form

$$D\left(\frac{\partial^4 w}{\partial x^4} + 2\frac{\partial^4 w}{\partial x^2 \partial y^2} + \frac{\partial^4 w}{\partial y^4}\right) + \sigma_x h \frac{\partial^2 w}{\partial x^2} + 2\tau h \frac{\partial^2 w}{\partial x \, \partial y} + \sigma y h \frac{\partial^2 w}{\partial y^2} = 0 \qquad (3.1)$$

where

$$D = \frac{Eh^3}{12(1 - \nu^2)} \qquad (3.2)$$

E   Young's modulus

h   plate thickness

ν Poisson's constant

w   displacement perpendicular to plate surface

σ_x, σ_y normal stresses along rectangular sides (positive, when compressive stresses)

τ shear stress along rectangular sides (just like σ_x and σ_y the positive direction for τ is opposite to that of normal convention)

Bleich (ref. 13) gives for the plate compressed in one direction ($\sigma_y = 0$, $\tau = 0$), loaded in the plastic range, after a kind of intuitive reasoning

$$D\left(\alpha \frac{\partial^4 w}{\partial x^4} + 2\sqrt{\alpha} \frac{\partial^4 w}{\partial x^2 \partial y^2} + \frac{\partial^4 w}{\partial y^4}\right) + \sigma_x h \frac{\partial^2 w}{\partial x^2} = 0 \qquad (3.3)$$

in which

$$\alpha = E_r/E \qquad (3.4)$$

the reduced modulus

$$E_r = \frac{4EE_t}{\left(\sqrt{E} + \sqrt{E_t}\right)^2} \tag{3.5}$$

just as it applies also to the buckling of rectangular bars (when assuming, as done in the past, that buckling is not coupled with progressive plastic deformation over the entire cross section) and D according to formula (3.2) hence with the elastic values for E and v.[3]

Chwalla (ref. 15) assumes that E can be replaced by $E_r = \alpha E$ and v by its plastic value v' in (3.1) and (3.2); in other words, that the plate remains isotropic. He reports that the elastic value can also be used, for $v < v' < 1/2$, and the variation in $1 - v^2$ does not amount to much.

When $v = v'$ it naturally follows that

$$\bar{\sigma}_x = \alpha \bar{\sigma}_{x,e} \tag{3.6}$$

where $\bar{\sigma}_x$ is the critical value of σ_x for the appearance of buckling, and $\bar{\sigma}_{x,e}$ the value as computed by elasticity theory. In consequence, Young's modulus E can be replaced by the reduced modulus E_r according to (3.5) in the formulas for the elastic range.

Timoshenko discussed the points of view of Bleich and Chwalla in reference 14.

The concepts of Bleich and Chwalla were not based upon specific laws of plastic deformation, but were obviously intended as a rough intuitive and safe approximation. Still, the reprinting of references 13, 14, and 15 following the publication of Nádai's book (ref. 16), with its simplest form of deformation theory for a hardened material, which, with all its defects, nevertheless proceeds from explicit assumptions, in conjunction with other findings (section 3.3) resulted in a more rigorously developed theory for the calculation of the critical buckling load of plates.

---

[3]Many writers take Poisson's transverse contraction coefficient v, so that it varies in the plastic range, and at progressive plastic deformation approaches 1/2 (since plastic volume change cannot occur). However, it is desirable to restrict v to the elastic part of the deformation, so that both v and E remain constant. The first-mentioned transverse contraction coefficient which thus refers to total deformation is expressed here by v'.

In Shanley's latest point of view, Bleich, Chwalla, and Timoshenko should not have employed the reduced modulus E_r but the tangent modulus E_t. Thus, according to Chwalla, E_t should replace E for the critical load $\bar{\sigma}_x$ in the formulas by elasticity theory. This suggestion was already made by Langhaar (ref. 17). The results obtained would, in consequence, be too low (except when the elastic limit itself is not yet exceeded), hence would give a much too unfavorable presentation of the subject.

Kollbrunner's method (ref. 8) lies about midway between that of Bleich and Chwalla, as seen from his differential equation

$$D \left\{ \alpha \frac{\partial^4 w}{\partial x^4} + \left(\alpha + \sqrt{\alpha} \right) \frac{\partial^4 w}{\partial x^2 \partial y^2} + \frac{\partial^4 w}{\partial y^4} \right\} + \sigma_x h \frac{\partial^2 w}{\partial x^2} = 0 \qquad (3.7)$$

Lastly, in order to check the agreement of his tests (section 4.3) with the thus developed theory, he introduced a rather arbitrary correction factor in the final critical load formulas.

Lundquist (ref. 18) also used a formula of Chwalla (3.6) but with α replaced by a correction factor, while

$$\beta = \frac{\alpha + 3\sqrt{\alpha}}{4}$$

This is intended as a kind of average of the aforementioned theories.

Gerard (ref. 19) substituted the secant modulus E_s for E in the formulas by elasticity theory, without, however, giving a more or less theoretical basis like the aforementioned writers. According to Gerard's method, it can be shown that the critical state of deformation of the plate in a certain load case is independent of the stress-strain relations. In figure 2.3 the curve by Gerard's method is shown as the stress-strain curve of the material.

3.3. DEFORMATION THEORY

Ilyushin (ref. 20) treated the stability of plates by deformation theory in its simplest form (briefly indicated by deformation theory, because more general deformation theories are not involved here) i.e., with Nádai's formulas (ref. 16) where $\nu = 1/2$, and with Shanley effect disregarded.

Kollbrunner, after his attempts discussed earlier (ref. 8), became immediately very enthusiastic and in reference 11 reexamines his own tests of reference 8 in the light of Ilyushin's report. He writes "The work of Ilyushin is theoretically correct and generally valid," but it was a premature conclusion. A disproval of incremental theories is not given; they are not even mentioned.

Stowell (ref. 21) deals with the work of Ilyushin, still uses $\nu = 1/2$, but includes the Shanley effect.

Bijlaard (ref. 22) gives the treatment of the stability of plates with the correct (elastic) value for ν and allows for the Shanley effect. Although his theory has not been generally known before this publication, it already had been published in different form in 1938 (in ref. 23), hence before the Shanley report (ref. 12).

Subsequently Stowell (together with Pride) supplemented his work (ref. 21) with other values of ν (ref. 24). With this he then got the same results as Bijlaard in the earlier report (ref. 22). Stowell compared the results of this report (ref. 24) with those of his report (ref. 21); the differences seem to be very small. Bijlaard, however, indicates (in ref. 25) that the correction by reference 24 or reference 21 for one of the two load cases investigated by Stowell has the opposite sign.

3.4. INCREMENTAL THEORIES

Handelman and Prager (ref. 9) applied Prager's incremental theory in its simplest form (in ref. 26, this theory is called incremental theory, for short; more general incremental theories are disregarded) to the buckling of plates without due regards to the Shanley effect. The exact value for ν is used.

Hopkins (ref. 27), Pearson (ref. 28, for $\nu = 1/2$) and Besseling (ref. 1) do this, while taking the Shanley effect into consideration. These last three reports should be regarded as being founded on the best theoretical basis.

3.5. DIFFERENCE BETWEEN DEFORMATION AND INCREMENTAL THEORY

EFFECT OF INITIAL ECCENTRICITY

3.5.1. Stress-Strain Relations

After, say, a hollow tube is stressed in tension or compression in the plastic range with a stress σ_0, an addition of torsion produces a distinct difference between deformation theory and incremental theory.

If, for instance, after simple tension or compression, while the stress σ remains constant, an increasing shear stress τ is added, the differential quotient $d\gamma/d\tau$ by deformation theory (for proof see supplement (A.3) is

$$\frac{d\gamma}{d\tau} = \frac{2\nu - 1}{E} + \frac{3}{E_t} + \frac{3\sigma_0}{\sqrt{\sigma_0{}^2 + 3\tau^2}}\left(1 - \frac{3\tau^2}{\sigma_0{}^2 + 3\tau^2}\right)\left(\frac{1}{E_{sec}(\sigma_0)} - \frac{1}{E_t}\right) \qquad (3.8)$$

$E_{sec}(\sigma_0)$ the secant modulus for stress σ_0.

By incremental theory (for proof see ref. 7 or supplement (A.2)

$$\frac{d\gamma}{d\tau} = \frac{2(1 + \nu)}{E} + \frac{9\tau^2}{\sigma_0{}^2 + 3\tau^2}\left(\frac{1}{E_t} - \frac{1}{E}\right) \qquad (3.9)$$

Originally, i.e. at $\tau = 0$, the aforementioned differential quotients have the values

$$\text{Deformation theory:} \quad \frac{d\gamma}{d\tau} = \frac{2\nu - 1}{E} + \frac{3}{E_{sec}(\sigma_0)} \qquad (3.10)$$

$$\text{Incremental theory:} \quad \frac{d\gamma}{d\tau} = \frac{2(1 + \nu)}{E} \qquad (3.11)$$

By (3.10) the behavior is inelastic, by (3.11) elastic, hence a considerable difference between the two theories. The elastic behavior according to (3.11), that is to say, according to (3.9) at $\tau = 0$, does not continue very long, as a rule, at increasing τ, for the fraction $1/E_t$ is generally great, and even infinitely great for the non-hardened or no longer hardened material.

But the differential quotient $d\gamma/d\tau$ for compressed plates is usually related in a large measure to the critical load condition.

Critical loads computed by incremental theory are always consider- ably higher than the experiment indicates. Calculations by deformation theory are usually in good agreement with the experiment. The failure of incremental theory is chiefly attributed to initial eccentricity. Therefore, shear stresses occur on a compressed plate before a critical load condition is reached.

An explanation for the fact that experimental values for critical loads are in good agreement with deformation theory (initial eccentricity discounted) might be found by attempting to point out that the differential quotient $d\gamma/d\tau$ in (3.9), by incremental theory, already assumes, at com- paratively small values of τ, a value equal to the value obtained by deformation theory at $\tau = 0$ according to (3.10).

If, viewed from the physical point of view, deformation theory is to give the correct stress-strain relations, then $d\gamma/d\tau$ should show con- siderable independence of τ according to (3.8). Deformation theory gives good results even without allowing for initial eccentricity.

Tables 3.1 to 3.8 show values for the differential quotients

$$E\left(\frac{d\gamma}{d\tau}\right)_F \quad \text{and} \quad E\left(\frac{d\gamma}{d\tau}\right)_D$$

by incremental and deformation theory, i.e. (3.9) and (3.8). The eight tables apply to eight different values of E_t, while $v = 0.3$. Each table shows seven values for the shearing stress τ. In the choice of the values for $E_{sec}(\sigma_0)$, of which $E(d\gamma/d\tau)_D$ alone is dependent

$$E_{sec}(\sigma_0) > E_t$$

must, of course, be valid.

Definite conclusions are difficult to draw. At increasing τ, $E(d\gamma/d\tau)_F$ remains, in most cases, considerably below the corresponding value $E(d\gamma/d\tau)_D$, at $\tau = 0$ (compare the numbers of the first column in each table with the number on top of the other columns). For the small values of E_t, paired with high $E_{sec}(\sigma_0)$ only, and not too low τ, the opposite is the case (cf. table 3.7 for $E_t = 0.02E$ and compare $E(d\gamma/d\tau)_F$ at $\tau = 0.03\sigma_0$ with $E(d\gamma/d\tau)_D$ at $E_{sec} = 0.9E$ and $\tau = 0$).

For the rest it is known that

$$\left(\frac{d\gamma}{d\tau}\right)_F = \left(\frac{d\gamma}{d\tau}\right)_D$$

at $E_{sec}(\sigma_0) = E$ (hence at $\sigma_0 = \sigma_e$, the proportional limit) and $\tau = 0$, which is seen from the tables, and up to what result the other numerical values of the tables must converge.

The quotient $E(d\gamma/d\tau)_D$ does not always increase much slower with increasing τ than $E(d\gamma/d\tau)_F$; for high values of $E_{sec}(\sigma_0)$ the process is even faster, as seen, when comparing the first column in table 3.7 with the other columns.

3.5.2. The Buckling Case of Onat and Drucker

From the foregoing (3.5.1) it is readily apparent that the discussion of stress-strain relations alone affords but a partial answer for predicting the experimental critical load by incremental theory.

Now, Onat and Drucker (ref. 7) made some calculations on an idealized case of torsional buckling of a cylindrical structure consisting of flat plates, so that the perpendicular section represents the form of a hollow cruciform. (See fig. 3.1 for section, figs. 3.2 and 3.3 for bar in straight and twisted state.) The elastic limit for compressive stress is $\sigma*$. Above it the tangent modulus is constant and has the value which follows from

$$20 = \frac{3G}{E_t} + 1 - \frac{3G}{E} \tag{3.12}$$

$$E_t = 0.05725E \quad \text{when} \quad \nu = 0.3 \tag{3.13}$$

The bar is so dimensioned that the critical compressive stress for torsional buckling, in the absence of initial eccentricity (i.e. of initial twist), is by elasticity theory

$$\bar{\sigma} = 2\sigma* \tag{3.14}$$

This is, at the same time, the value obtained by incremental theory. Deformation theory gives, however

$$\bar{\sigma} = 1.05\sigma* \tag{3.15}$$

This result is calculated in supplement B. (In ref. 7 this value appears only in a plot.) Supplement B shows at the same time that $E_{sec}(\bar{\sigma})$ with $\bar{\sigma}$ given by (3.15) is equal to

$$E_{sec} = 0.560E \quad \text{when} \quad \nu = 0.3 \tag{3.16}$$

With the inclusion of an initial eccentricity in the calculation, the definition of what is considered as buckling load is naturally somewhat arbitrary. In the case in point the maximum load which the bar is able to sustain (even without eccentricity the critical load is at the same time the maximum load) can be taken for this purpose.

As initial angle of twist per length 2b of the section 0.000111, 0.00111, and 0.0111 rad. is successively used. The divers results are found in table 3.9 (computed with the data of figure 9 from ref. 7).

With this it is proved that, when proceeding from incremental theory, even a slight initial eccentricity is sufficient to produce a considerable displacement of the computed critical load and that the value of it is comparatively little dependent on the initial eccentricity (naturally only for an eccentricity already different from zero). The thus computed critical loads are close to those obtained by deformation theory with and without initial twist, for there is very little difference between them.

The unusual feature of the Onat and Drucker load case is that in spite of the presence of initial twist, the state of stress remains uniform during the application of the load. In other problems on plates which have an initial eccentricity, this is not the case as a rule, and problems such as these are very little amenable to calculation. However, it is to be expected that then specific changes in the critical buckling load (which then indicates the load at which, more or less suddenly, the deflection assumes a significant form) will occur.

Whether these changes will then show the same degree of independence from the actual amount of initial eccentricity, and whether the data then are again in close agreement with deformation theory (without counting initial eccentricity) has, of course, not been established as yet. It is not known even in the particular load case of Onat and Drucker for

values of the tangent modulus different from those which they used, and which is rather at the lower limit ($E_t \sim 0.05E$) or for other dimensions of the structure.

In this buckling case the stress-strain relations themselves exhibit the marked effect of initial eccentricity. (Cf. table 3.6 at $E_t = 0.05E$.) (In (3.13) $E_t = 0.05725E$.)

At $\tau = 0.1\sigma_0$

$$E(d\gamma/d\tau)_F = 4.260$$

hence substantially higher than that at $\tau = 0$ (2.600).

At a τ value only slightly above $\tau = 0.1\sigma_0$ the value obtained for $E(d\gamma/d\tau)_F$ is equal to $E(d\gamma/d\tau)_D$ at $\tau = 0$ and $E_{sec}(\sigma_0) = 0.5E$ (in (3.16), $E_{sec}(\sigma_0) = 0.560E$).

However, it already has been proved that for other values of E_t and $E_{sec}(\sigma_0)$ the quotient $E(d\gamma/d\tau)_F$ increases slower at increasing τ and reaches the value of $E(d\gamma/d\tau)_D$ at $\tau = 0$ not until later. Nevertheless, the buckling case of Onat and Drucker gives a good qualitative picture of the influence of initial eccentricities.

Bijlaard and Wiseman likewise point out (in ref. 46) that the approximate coincidence of the results by incremental theory, when initial eccentricity is allowed for, with those by deformation theory (initial eccentricity disregarded) in the Onat and Drucker buckling case is not applicable to other relations.

That, all the same, deformation theory is always in agreement with experiment, as Bijlaard and Wiseman claim (cf. section 4.1), must have been known to them from the fact that incremental theory is not correct, but that deformation theory is valid, at least at load changes such as occur in buckling cases and where the data of the theory of Batdorf and Budiansky are equal to that of a deformation theory (not that by Nádai, compare section 3.3). (See section 10.1 of ref. 3, for example.)

Bijlaard and Wiseman conclude their discussion of reference 7 with: "Nevertheless, it is a welcome contribution for indicating that small divergences in the direction of incremental theory are cancelled by initial eccentricities."

3.6. COMPARISON OF DATA FOR CRITICAL LOADS BY DEFORMATION

AND INCREMENTAL THEORY

Such a comparison is shown in figure 3.4, taken from reference 1.
The reproduction of four load cases is the same as discussed in sec-
tion 2.3.2.3.

The dashed curves represent deformation theory, the solid curves
incremental theory, both allowing for the Shanley effect. The plot
also shows to which load cases the respective curves refer.

Figures 3.5 and 3.6, taken from reference 9, give the same data as
figure 2.1. The variation of the buckling factor k is plotted verti-
cally, the ratio a/b of the sides of the rectangular plate hinged
along all edges, horizontally. The plate is loaded on the side of
length b in compression in one direction.

· Figure 3.5 represents the curves by incremental theory and, according
to Bleich, both computed without the Shanley effect. The curve by elas-
ticity theory is also shown. All curves were computed with consideration
to the exact elastic value for the transverse contraction coefficient
$\nu = 0.32$.

Because Handelman and Prager wanted to compare their results with
that of Ilyushin, they computed the data with $\nu = 1/2$. The particular
comparison is shown in figure 3.6.

Figures 3.7, taken from reference 30, and 3.8, taken in part from
reference 30 and in part from reference 31, represent the data of several
theories for an infinitely long plate hinged along the edges compressed
in length direction. The shape of figure 3.7 is that according to fig-
ure 2.4, that of figure 3.8 according to figure 2.3.

The results of the several methods based on deformation theory are
not far from each other and near the curve according to Gerard's method.
The inclusion or exclusion of the Shanley effect does not matter much.
(Compare Ilyushin's curves in figs. 3.7 and 3.8 with that by Stowell in
the same plots.)

Incremental theory gives consistently much higher data than defor-
mation theory or Gerard's method. Whether the Shanley effect is included
or not, does not matter much. Compare the Handelman and Prager curves in
figure 3.8 with those of Bijlaard (in ref. 31) by incremental theory,
computed with Shanley effect accounted for.

4. EXPERIMENTAL DATA

4.1. NACA TESTS

Of the NACA tests for 1945-1946, while the present report was written, references 32, 33, 34, 35, and 36 were available. These experiments deserve special attention since Bijlaard in reference 23 sees in the results of these experiments a confirmation of deformation theory.

They are compression tests on H, Z, and channel sections. The section forms used, as described in reference 32, are found in figure 4.1, those of references 33 to 36 in figure 4.2. The dimensions of the columns were so chosen that column buckling did not occur, but only local instability. In references 33 to 36 it is stated that: "The lengths of the columns were selected so as to obtain whenever possible a desirable three-half wave buckling pattern." In the description of the tests nothing is ever mentioned about the buckling pattern in flanges or webs, only the critical load is indicated. The cross-sectional distortion of the sections according to figure 4.1 is given once. (See fig. 4.3.)

The selfsame photograph of an H-section under compression published in references 31 to 36 shows buckled flanges. The buckling pattern is so laid out that it consists of three-half waves. The photograph shows no sign of web buckling. About the condition of the critical load the following statement is given: "In the local instability test, measurements were taken of the cross-sectional distortion, and the critical stress was determined as the stress at the point near the top of the knee of the stress-distortion curve where a marked increase in distortion first occurred with small increase of stress." It is well known that such methods of determining the buckling load contain a large measure of arbitrariness. (See ref. 48, for example.)

In the tests of references 32 to 36 stress-strain curves are determined on test pieces taken on different areas of the cross section. In each of the cited publications, either an average diagram is given which indicates the amount of scattering over all test pieces, or 5 to 10 diagrams, which again were the averaged result of a number of test specimens from the same section bar. What seems to be about the extreme limit of the thus published stress-strain curves is represented in figure 4.4 to figure 4.7. It is seen then that Gerard's method (section 3.2) always gives somewhat higher results. The writers themselves apply no theory. Figures 4.4 to 4.7 simply contain curves which indicate the average location of the test points.

Reference 38 again discusses the results of the NACA tests of reference 33, as far as the H-sections are concerned. Figure 4.8 represents

experimental points in a diagram of the form of figure 2.3. The calcu-
lation of the critical load by elasticity theory is carried out according
to reference 40. Theoretical curves are also shown. The theoretical
critical loads in the plastic range are likewise computed according to
the principles of reference 40 and with the aid of Stowell's report
(ref. 21).

A summary of references 32 to 36 is given in reference 39. From
this reference 39 it is apparent that references 44 and 45 belong in
the test series of references 32 to 36. The last-named reports were not
available, however, to the writer at the time this report was written.

Bijlaard (in ref. 22) gives the diagram on figure 4.9, in which the
curves for two load cases computed by deformation theory are shown.[4]
Then, he quotes "NACA tests 1945-1946." Of what tests precisely, is not
mentioned. It is certain that the material was "avional," but which of
the materials used by Pride and Heimerl was meant by it? The quotes are
not immediately traceable to the work of Pride and Heimerl. Neither is
the stress-strain curve for "avional," which was copied by Bijlaard with-
out the scatter of Heimerl and Pride. (A line is drawn through the eight
points of figure 4.9 in reference 22, but that is no theoretical curve;
it merely indicates an averaged position of the intended points.) Appar-
ently Bijlaard did not compute the critical load by elasticity theory
again, but simply followed the report of Pride and Heimerl.

If, in the NACA tests, the flanges really have started to buckle, the
values of the critical load should lie between load cases I and II, at
least on the premise that the buckling flanges in the tests are still
considered as infinitely long (three half-wave waves occur, according
to fig. 4.9). But even Gerard's simple rule itself yields results which
are fairly accurate, for the experimental points are located near to the
stress-strain curve of figure 4.9.

Pride and Heimerl (ref. 30) also made some compression tests on a
long, square, hollow, seamless box. The individual plates could then
be considered as simply supported at the edges.

Figure 4.10 represents test points for seven groups of test pieces,
each group referring to test pieces from one sectional bar. Besides the
test points, the curves of Gerard, i.e. stress-strain curves, are plotted.
There still is some scattering between the stress-strain curves of the
different groups. And even within a group of test pieces from one bar
the scatter is fairly wide. (Cf. the limits indicated on curve C.)

---

[4]The support conditions of the ends infinitely far from each other is
of no significance. For case II, in which ∞ waves occur, this is instantly
clear. In case I a half-wave occurs for hinged ends; for clamped ends,
a whole wave. But in this case the critical compressive load is indepen-
dent of the wave length, if the wave length is great.

The same measurements are repeated in figure 4.11, but after correction (according to ref. 47), hence refer to material with a constant stress-strain curve. The theoretical curves are those of figure 3.5. The agreement with Stowell's theory is good. Gerard's secant-modulus method should also give acceptable results.

4.2. GERARD'S EXPERIMENTS

Gerard (ref. 19) likewise made some tests on Z and channel sections and established a satisfactory proof of his secant modulus method. The chart in which the real critical load is plotted against the calculation by elasticity theory obtained by secant modulus method, passes nicely along the test points. (See fig. 4.12 and fig. 4.13.) The calculation of the critical load by elasticity theory was made according to reference 41. One noticeable feature of figure 4.13 is that the agreement between theory and experiment in the elastic range is not good, which raises some doubt as to whether all experiments are not at the upper limit. The true critical load is determined from the difference in strain at the opposite sides of a flange. At first the difference seems to be practically zero, but at incipient buckling this difference grows quickly at slightly increasing mean compressive stress (fig. 4.14). Figures 4.12 and 4.13 also show the curves according to Lundquist (ref. 18) and Langhaar (ref. 17) (tangent modulus method).

Other tests by Gerard are reported in reference 42 and discussed also by Stowell (in ref. 43). The tests refer to a shearing test on an infinitely long rectangular plate. The long edges of the plate are rigidly clamped. Reference 43 gives a diagram in which the critical shearing stress is plotted against the critical shearing strain computed by elasticity method, according to Stowell's theory and Gerard's secant modulus method (fig. 4.15). Gerard's curve forms the shearing stress-shearing strain curve of the material. Stowell's curve can also be applied to the case of hinged long sides. (Naturally, that of Gerard is too.)

This case was also treated by Stowell, but there was only a very small difference from the case of clamped edges, which cannot be taken into account in the calculation.

The agreement between the experimental evidence and the curve by Gerard's method is not as good in figure 4.15 as in figures 4.12 and 4.13.[5]

---

[5]Translator's note: Figure 4.15, taken from reference 43, appears to be in error and is misleading, Gerard's method actually gives lower stresses than Stowell's method. (See NACA TN 3184.)

4.3. Kollbrunner's Experiments

In reference 8 Kollbrunner investigated rectangular plates of different length/width ratios for several load cases (fig. 4.16). The edges of length b were assumed to be hinge supported, those of length a free, hinge supported or clamped, as illustrated in figure 4.16. The tests were made on perfectly simple plates; thus, for example, the plate for case II (fig. 4.14) was not the flange of an equilateral angle section loaded in compression nor the plate of case IV a side of a square box beam, such as the other investigators used.

Figure 4.17 shows a portion of Kollbrunner's setup. The lateral edges of the plates are enclosed in small steel tabs, which safeguarded the hinged support of the edges as illustrated in figure 4.18(a). The set screws in the steel tabs insured clamping (fig. 4.18(b)).

Kollbrunner checked his experimental results against his theoretical solutions obtained by the differential equation (3.7) which is a kind of mean of Bleich's and Chwalla's relations.

The theoretical result for the critical compressive stress $\bar{\sigma}$ is

$$\bar{\sigma} = p\,\frac{\pi^2 E}{12\left(1-\nu^2\right)}\left(\frac{h}{b}\right)^2\frac{\alpha+\sqrt{\alpha}}{2}+\frac{1}{K}\,q\,\frac{\pi^2 E}{12\left(1-\nu^2\right)}\left(\frac{ha}{b^2}\right)^2\frac{1}{m^2}+$$

$$K\,\frac{\pi^2 E}{12\left(1-\nu^2\right)}\left(\frac{h}{a}\right)^2 m^2\alpha \tag{4.1}$$

with

a   plate length

b   plate width

h   plate thickness

α   by (3.4) and (3.5)

m   number of half-waves of buckling pattern

The constants p and q in the different load cases (fig. 4.16) have the following values:

Case			
I		p = 0	q = 0
II		p = 0.425	q = 0
III		p = 0.570	q = 0.125
IV		p = 2	q = 1
V		p = 2.5	q = 5
VI		p = 2.270	q = 2.450

Coefficient K in (4.1) is a correction factor defined by experiment. The neccessity for the use of this coefficient is attributable to the fact that the assumption of hinged plate support on the short side where they are compressed is not perfect, since small bending moments can still be taken up here.

The correction factor K for case I is not given. For case II a factor K = 1.5 should be applicable in the elastic as well as in the plastic range. For cases III to VI a factor K = 1.2 is applicable, but in the plastic range only.

By (4.1) it can be deduced that the critical compressive stress $\bar{\sigma}$ for the infinitely long plate is

$$\bar{\sigma} = \frac{\pi^2 E \sqrt{\alpha}}{12\left(1 - \nu^2\right)} \left(\frac{h}{b}\right)^2 \left[p \, \frac{1 + \sqrt{\alpha}}{2} + 2\sqrt{q} \right] \qquad (4.2)$$

as given by Kollbrunner himself.

Coefficient K does not appear any longer in (4.2), and actually, the manner of support of ends loaded infinitely far from each other are of no interest in load cases II to VI. Compare case II with case I mentioned in the footnote of section 4.1.

Kollbrunner does not report why the factor K = 1.5 for case I holds in the elastic and the plastic range, whereas for cases III to VI the factor K, which, moreover, has another value, is valid in the plastic range only. All the same the use of the correction factor K seems a rather arbitrary interference in the experimental check of a theory which itself has as yet no solid basis. (Cf. section 3.2.) On top of that, it should be remembered that the significance of K decreases considerably when long plates are involved. The figures 4.19, 4.20, and 4.21, of the same pattern as figure 2.1, represent some test data with the "theoretical"

curves, i.e. curves obtained with correction factor K, together with the curves of Bleich and Chwalla and Kollbrunner, respectively, of references 13 and 15. These graphs still show points which are up to 10 percent lower than Kollbrunner's "theoretical" curves, which Kollbrunner, indeed, confirms in reference 11.

To define the instant of buckling, a straight bar is reflected in the plate surface. According to Kollbrunner, "the instant of buckling was momentarily plainly visible by a typical jump of the reflected bar from its straight shape into the wave pattern."

After the appearance of reference 20, Kollbrunner becomes a supporter of Ilyushin's theory, to which he subscribes, as stated before, with great enthusiasm in reference 11. Ilyushin's theory gives up to 10 percent higher values than Kollbrunner's theory, and the latter believes that if the correct (elastic value) is used instead of $\nu = 1/2$ in Ilyushin's theory, both theories would be in good agreement.

Figures 4.22 and 4.23, of the same form as figure 2.2, represent some experimental results, based on the theoretical curves of Kollbrunner and Ilyushin.

5. DISCUSSION

The deformation theory of plastic strain applied to the calculation of the critical buckling load of plates gives results which are in better agreement with experiment than incremental theory.

Onat and Drucker give an explanation for the failure of incremental theory in computing critical buckling loads for a special case by assuming an initial eccentricity.

Some writers consider deformation theory as "perfectly correct" and are willing to see more in it than a practical calculating rule. It never has been proved even for general cases that incremental theory applied to a plate with initial eccentricities gives exactly the same results as deformation theory applied to the plate, without counting with the initial eccentricity.

The statement of some writers that their or someone else's experiments are in "excellent agreement" with their own theory needs to be critically examined.

At such a pronouncement the question often arises:

1. How much scatter was there in the stress-strain curves? (Cf. the scattering in figs. 4.4 to 4.7, for example.)

2. Exactly how is the buckling limit defined? Compare, for example, references 32 to 36, where "the critical load is considered as reached, when the distortion of the cross section begins to show a rapid increase with slightly increasing stress."

3. Little scatter in the measured critical state of stress is no indication of whether there are disturbing secondary effects in the experiment or initial eccentricity. Groups of identical plates, loaded fairly far in the plastic range, almost all exhibit the same critical buckling load, but fairly far in the plastic range the tangent modulus E_t is usually small, and the stresses which can occur even before buckling can then still not vary very much. However, should not the scatter in distortions on reaching the critical state be much greater?

The information about these problems is generally very vague. Considering reference 30 as example (already discussed in section 4.1), the following may be stated:

To 1. The scattering in the stress-strain curves for one of the square boxes used as the test pieces seems to be considerable (fig. 4.10, curve C.) Between the mean curves for the different boxes there are differences of the same kind.

To 2. As examples of the determination of the buckling load two suitable diagrams are given in reference 30 (fig. 5.1). But they refer to cases in which the buckling load was, at the same time, approximately the maximum load. Diagrams for cases in which the maximum load was considerably above the buckling load were not given. In this connection the question arises as to how it was possible that on many tubes the buckling stress and the mean stress at maximum load were almost identical, but far below the 0.2 strain limit, as seen from table I of reference 30 (42.8 ksi, 43.2 ksi, and 61.4 ksi).

Lacking further information, this is a very remarkable result. The inescapable conclusion was that for a better insight into the problem we had to carry out experiments of our own.

6. CONCLUSIONS

1. It may be assumed that the plastic distortion increases even during buckling. Unloading according to elasticity theory is not required (Shanley effect).

2. The incremental theory of plastic deformation is really the one which should be applied to the calculation of critical buckling loads of plates.

3. Initial eccentricities are bound to have a marked displacement effect on the result. As a rule, however, it is practically impossible to allow for such eccentricities in the derivation.

4. Deformation theory applied without regard to initial eccentricities gives practical results.

5. Of all the writers starting from deformation theory, Bijlaard gives the best treatment. He accounts for the Shanley effect and introduces the correct value of the transverse contraction coefficient.

6. Uncertainties in the stress-strain curve at incipient buckling, likewise the scattering in the experiment, often show agreement between theory and experiment that seems better than it actually is.

7. The difference in theoretical results for the critical load on the basis of deformation theory with or without Shanley effect and with or without the correct value of ν is not or, not much, greater than the scattering that is to be observed as the result of many causes during the experiment.

8. Less explored is the critical distortion at which buckling occurs.

9. Gerard's method, which introduces the secant modulus, i.e. Young's modulus in the formulas for the buckling stress in the elastic range, always gives, it is true, a higher critical buckling stress than deformation theory, although it gives, nevertheless, a practical calculating rule.

10. A better insight into the problem involved may perhaps be obtainable by personal experimental investigation.

Translated by J. Vanier
National Advisory Committee
for Aeronautics

SUPPLEMENT A

THE DIFFERENTIAL QUOTIENT $d\gamma/d\tau$ OF INITIALLY SIMPLY

COMPRESSED MATERIAL AS FUNCTION OF THE LATER

ON ADDED SHEARING STRESS τ

A.1. INTRODUCTION

The material is such that above the elastic limit and at increasing load in a compression test the differential quotient $d\sigma/d\epsilon = E_t$ exhibits a constant value. The material is first considered as subjected to a compressive stress $\sigma = \sigma_0$, after which at constant σ, a shearing stress τ is added. The secant modulus on reaching compressive stress σ_0 is $E_{sec}(\sigma_0)$, hence, also a constant in the subsequent calculations.

A.2. BY FLOW THEORY

The formulas (11.16) and (11.17) of reference 3 give the stress-strain relations for the case that only normal stresses σ (positive if σ is a compressive stress) and shearing stresses τ are applied

$$d\epsilon = \frac{d\sigma}{E} + \frac{2}{3} p\sigma \, dJ_2 \qquad (A.1)$$

$$d\gamma = \frac{2(1 + \nu)}{E} \, d\tau + 2p\tau \, dJ_2 \qquad (A.2)$$

ϵ the normal strain (positive when ϵ is a compression).

$$J_2 = \frac{1}{3} \sigma^2 + \tau^2 \qquad (A.3)$$

and p is a function of J_2. First to be investigated is the function of J_2 on the basis of constant tangent modulus E_t in the compression test, where, because $\tau = 0$

$$J_2 = \frac{1}{3}\,\sigma^2 \qquad\qquad\qquad (A.4)$$

and by (A.1) and (A.3)

$$d\epsilon = \frac{d\sigma}{E} + \frac{2}{3}\,p\sigma\,\frac{2}{3}\,d\sigma = \frac{d\epsilon}{E_t} \qquad\qquad (A.5)$$

or

$$p = \frac{9}{4\sigma^2}\left(\frac{1}{E_t} - \frac{1}{E}\right)$$

and with (A.4)

$$p = \frac{3}{4J_2}\left(\frac{1}{E_t} - \frac{1}{E}\right) \qquad\qquad (A.6)$$

Formula (A.6), where $\sigma = \sigma_0$ and (A.6) are substituted in (A.2), gives

$$\frac{d\gamma}{d\tau} = \frac{2(1 + \nu)}{E} + \frac{9\tau^2}{\sigma_0^2 + 3\tau^2}\left(\frac{1}{E_t} - \frac{1}{E}\right) \qquad (A.7)$$

which is identical with (3.9) and at $\tau = 0$ changes to (3.11).

A.3. BY DEFORMATION THEORY

Formulas (11.14) and (11.15) of reference 3 give relations between stresses σ and τ and strains ϵ and γ

$$\epsilon = \frac{\sigma}{E} + \frac{2}{3}\,P\sigma \qquad\qquad\qquad (A.8)$$

$$\gamma = \frac{2(1 + \nu)}{E}\,\tau + P\tau \qquad\qquad (A.9)$$

with P a function of J_2 with J_2 according to (A.3).

Now assume that the equation of the stress-strain relation for the compressive test in the plastic range is

$$\epsilon = \frac{\sigma}{E_t} - a \qquad\qquad\qquad (A.10)$$

This, substituted in (A.8), gives

$$P = \frac{3}{2}\left(\frac{1}{E_t} - \frac{1}{E}\right) - \frac{3a}{2\sigma}$$

and since (A.4) is valid again for this test, P becomes

$$P = \frac{3}{2}\left(\frac{1}{E_t} - \frac{1}{E}\right) - \frac{3a}{2\sqrt{3J_2}} \qquad\qquad (A.11)$$

Formula (A.3) in which $\sigma = \sigma_0$ and (A.11) are substituted in (A.9) gives

$$\gamma = \frac{2(1 + \nu)}{E}\tau + 3\left(\frac{1}{E_t} - \frac{1}{E}\right)\tau - \frac{3a\tau}{\sqrt{\sigma_0^2 + 3\tau^2}} \qquad (A.12)$$

The constant a can be eliminated by ascertaining that after applying the compressive stress σ_0 according to (A.10)

$$\epsilon = \frac{\sigma_0}{E_{sec}(\sigma_0)} = \frac{\sigma_0}{E_t} - a$$

or

$$-a = \sigma_0\left(\frac{1}{E_{sec}(\sigma_0)} - \frac{1}{E_t}\right)$$

is valid, which in (A.12) gives

$$\gamma = \frac{2(1 + \nu)}{E}\tau + 3\left(\frac{1}{E_t} - \frac{1}{E}\right)\tau + \frac{3\sigma_0\tau}{\sqrt{\sigma_0^2 + 3\tau^2}}\left(\frac{1}{E_{sec}(\sigma_0)} - \frac{1}{E_t}\right) \qquad (A.13)$$

The differential quotient becomes

$$\frac{d\gamma}{d\tau} = \frac{2(1 + \nu)}{E} + \frac{3}{E_t} - \frac{3}{E} + \frac{3\sigma_0}{\sqrt{\sigma_0^2 + 3\tau^2}}\left[\left(1 - \frac{3\tau^2}{\sigma_0^2 + 3\tau^2}\right)\left(\frac{1}{E_{sec}(\sigma_0)} - \frac{1}{E_t}\right)\right]$$
$$(A.14)$$

hence is identical with (3.8) and at $\tau = 0$ becomes (3.10) and when $E_{sec}(\sigma_0) = E$, changes to (3.11).

SUPPLEMENT B

DETERMINATION BY DEFORMATION THEORY OF THE CRITICAL BUCKLING

LOAD OF THE ONAT AND DRUCKER LOAD CASE IN THE ABSENCE

OF INITIAL ECCENTRICITY AND PREDICTION OF THE

SECANT MODULUS FOR THIS LOAD

In the Onat and Drucker buckling case the yield point is $\sigma*$. The critical compressive load by elasticity theory is $\bar{\sigma}_e = 2\sigma*$. Above the yield point the tangential modulus E_t is assumed constant, and has the value that follows from

$$20 = \frac{3G}{E_t} + 1 - \frac{3G}{E} \tag{B.1}$$

hence $E_t = 0.05E$ for $\nu = 1/2$ and $E_t = 0.057E$ for $\nu = 0.3$.

Above the yield point the relation between compressive stress and compression is

$$\epsilon = \frac{\sigma}{E_t} - \frac{\sigma*}{E_t} - \frac{\sigma*}{E} \tag{B.2}$$

and the secant modulus is

$$E_{sec} = \frac{\sigma}{\dfrac{\sigma}{E_t} - \dfrac{\sigma*}{E_t} + \dfrac{\sigma*}{E}} \tag{B.3}$$

At small increase of shearing stress τ the differential quotient by deformation theory is identical with (3.10)

$$\frac{1}{G_{sec}} = \frac{d\gamma}{d\tau} = \frac{2\nu - 1}{E} + \frac{3}{\sigma}\left(\frac{\sigma}{E_t} - \frac{\sigma*}{E_t} + \frac{\sigma*}{E}\right) \tag{B.4}$$

For the special load case in question the critical value of σ by incremental theory has the value according to elasticity theory, hence $\bar{\sigma} = \bar{\sigma}_e = 2\sigma*$, as long as no initial deflections exist.

The critical value for σ by deformation theory becomes

$$\sigma_e = \frac{G_{sec}}{G} \bar{\sigma}_e = \frac{2G_{sec}}{G} \sigma^*$$ (B.5)

In view of (A.18) and (A.19), the value of $\bar{\sigma}$ is the solution for σ from the equation

$$\frac{\sigma^*}{\sigma} = \frac{G}{2}\left(\frac{2\nu - 1}{E} + \frac{3}{E_t} - \frac{3}{E_t}\frac{\sigma^*}{\sigma} + \frac{3}{E}\frac{\sigma^*}{\sigma}\right)$$

$$\bar{\sigma} = \frac{\frac{2}{G} + \frac{3}{E_t} - \frac{3}{E}}{\frac{2\nu - 1}{E} + \frac{3}{E_t}} = \frac{1}{\frac{3G}{E_t} + 1 - \frac{3G}{E}} + 1$$ (B.6)

and with (B.1)

$$\bar{\sigma} = 1.05\sigma^*$$

When the compressive stress reaches this value, the secant modulus is, by (B.3) and (B.1)

$$E_{sec} = 0.525E \quad \text{for} \quad \nu = 1/2$$

$$E_{sec} = 0.560E \quad \text{for} \quad \nu = 0.3$$

REFERENCES

1. Besseling, J. F.: Over het knikvraagstuk in het plastische gebied
   bij staven en platen. Deel I. N.L.L. Rapport S.407, 1952.

2. Prager, W.: The Stress-Strain Laws of the Mathematical Theory of
   Plasticity — A Survey of Recent Progress. Jour. Appl. Mech.,
   vol. 15, no. 3, Sept. 1948, pp. 226-233.

3. Benthem, J. P.: On the Stress-Strain Relations of Plastic Deformation.
   N.L.L. Report S.398, 1951.

4. Besseling, J. F.: A Theory of Plastic Flow for Anisotropic Hardening
   in Plastic Deformation for an Initially Isotropic Material. N.L.L.
   Report S.410, 1954.

5. Prager, W.: Recent Contributions to the Theory of Plasticity. Applied
   Mechanics Reviews, vol. 4, no. 11, Nov. 1951, p. 585.

6. Batdorf, S. B., and Budiansky, Bernard: A Mathematical Theory of
   Plasticity Based on the Concept of Slip. NACA TN 1871, 1949.

7. Onat, E. T., and Drucker, D. C.: Inelastic Instability and Incremental
   Theory of Plasticity. Jour. Aero. Sci., vol. 20, no. 3, Mar. 1953,
   pp. 181-186.

8. Kollbrunner, C. F.: Das Ausbeulen der auf einseitigen, gleichmässig
   verteilten Druck beanspruchten Platten im elastischen und plastischen
   Bereich. Mitt. no. 17, Inst. für Baustatik an der E.T.H., Gebr.
   Leeman & Co., (Zurich), 1946.

9. Handelman, G. H., and Prager, W.: Plastic Buckling of a Rectangular
   Plate Under Edge Thrusts. NACA Rep. 946, 1949.

10. Schuette, E. H., and McDonald, J. C.: Prediction and Reduction to
    Minimum Properties of Plate Compressive Curves. Jour. Aero. Sci.,
    vol. 15, no. 1, Jan. 1948, p. 23.

11. Kollbrunner, C. F., and Hermann, G.: Stabilität der Platten im
    plastischen Bereich. Mitt. no. 20 aus dem Inst. für Baustatik a/d
    Eidgen. Technischen Hochschule in Zurich, 1947.

12. Shanley, F. R.: Inelastic Column Theory. Jour. Aero. Sci., vol. 14,
    no. 5, May 1947, pp. 261-267.

13. Bleich, F.: Theorie und Berechnung der eisernen Brücken, Berlin 1924,
    S. 220. Ook: Vorbericht zum I. Internat. Kongr. f. Bruckenbau und
    Hochbau in Paris 1932, p. 109.

14. Timoshenko, S.: Theory of Elastic Stability. McGraw-Hill Book Co., Inc., 1936, p. 384.

15. Chwalla, E.: Das allgemeine Stabilitätsproblem der gedrückten, durch Randwinkel verstärkten Platte. Ing.-Archiv, Bd. V, Heft 1, Feb. 1934, pp. 54-65.

16. Nádai, A.: Plasticity. McGraw-Hill Book Co., Inc., 1931.

17. Langhaar, H. L.: Buckling of Aluminum-Alloy Columns and Plates. Jour. Aero. Sci., vol. 10, 1943, p. 218.

18. Lundquist, Eugene E.: Local Instability of Symmetrical Rectangular Tubes Under Axial Compression. NACA TN 686, 1939.

19. Gerard, George: Secant Modulus Method for Determining Plate Instability Above the Proportional Limit. Jour. Aero. Sci., vol. 13, no. 1, Jan. 1946, pp. 38-44 and 48.

20. Ilyushin, A. A.: The Elasto-Plastic Stability of Plates. NACA TN 1188, 1947.

21. Stowell, Elbridge Z.: A Unified Theory of Plastic Buckling of Columns and Plates. NACA Rep. 898, 1948. (Supersedes NACA TN 1556.)

22. Bijlaard, P. P.: Theory and Tests on the Plastic Stability of Plates and Shells. Jour. Aero. Sci., vol. 16, no. 9, Sept. 1949, pp. 529-541.

23. Bijlaard, P. P.: A Theory of Plastic Stability and Its Application to Thin Plates of Structural Steel. Knoinklijke Nederlandsche Akad. Wetenschappen. Reprinted from Proc., vol. XLI, no. 7, 1938, pp. 731-743.

24. Stowell, Elbridge Z., and Pride, Richard A.: The Effect of Compressibility of the Material on Plastic Buckling Stresses. Jour. Aero. Sci., vol. 18, no. 11, Nov. 1951, p. 773.

25. Bijlaard, P. P.: Taking Account of the Compressibility of the Material in the Plastic Buckling of Plates. Jour. Aero. Sci., vol. 19, July 1952, p. 493.

26. Prager, W.: On Isotropic Materials With Continuous Transition From Elastic to Plastic State. Proc. of the 5th. Int. Congress of Appl. Mech. Cambridge Mass., 1938, p. 234.

27. Hopkins, H. G.: Plastic Deformation of Rectangular Plates Under Direct Loads. Engineering Structures, p. 93. Special Supplement to Research. London, Butterworths Scientific Publications, 1949.

28. Pearson, C. E.: Bifurcation Criterion and Plastic Buckling of Plates
    and Columns. Jour. Aero. Sci., vol. 17, no. 7, July 1950,
    pp. 417-424, 455.

29. Peters, Roger W., Dow, Norris F., and Batdorf, S. B.: Preliminary
    Experiments for Testing Basic Assumptions of Plasticity Theories.
    Proc. Soc. Exp. Stress Analysis, vol. 7, no. 2, (presented at the
    Spring meeting, May 1949.)

30. Pride, Richard A., and Heimerl, George J.: Plastic Buckling of
    Simply Supported Compressed Plates. NACA TN 1817, 1949.

31. Bijlaard, P. P.: On the Plastic Buckling of Plates According to the
    Flow Theory. Jour. Aero. Sci., vol. 17, 1950, p. 810.

32. Heimerl, George J., and Roy, J. Albert. Column and Plate Compressive
    Strengths of Aircraft Structural Materials. 17S-T Aluminum-Alloy
    Sheet. NACA WR L-20, 1945. (Formerly NACA ARR L5F08.)

33. Heimerl, George J., and Roy, J. Albert: Column and Plate Compressive
    Strengths of Aircraft Structural Materials. Extruded 75S-T Alumi-
    nium Alloy. NACA WR L-173, 1945. (Formerly NACA ARR L5F08a.)

34. Heimerl, George J., and Roy, J. Albert: Column and Plate Compressive
    Strengths of Aircraft Structural Materials. Extruded 24S-T Alumi-
    nium Alloy. NACA WR L-32, 1945. (Formerly NACA ARR L5F08b.)

35. Heimerl, George J., and Fay, Douglas P.: Column and Plate Compressive
    Strengths of Aircraft Structural Materials. Extruded R303-T Alumi-
    nium Alloy. NACA WR L-33, 1945. (Formerly NACA ARR L5H04.)

36. Heimerl, George J., and Niles, Donald E.: Column and Plate Compres-
    sive Strengths of Aircraft Structural Materials. Extruded 14S-T
    Aluminium Alloy. NACA ARR L6C19, 1946.

37. Kroll, W. D., Fisher, Gordon P., and Heimerl, George J.: Charts for
    Calculation of the Critical Stress for Local Instability of Columns
    With I-, Z-, Channel, and Rectangular-Tube Section. NACA WR L-429,
    1943. (Formerly NACA ARR 3K04.)

38. Stowell, Elbridge Z., and Pride, Richard A.: Plastic Buckling of
    Extruded Composite Sections in Compression. NACA TN 1971, 1949.

39. Heimerl, George J.: Determination of Plate Compressive Strengths.
    NACA TN 1480, 1947.

40. Lundquist, Eugene E., Stowell, Elbridge Z., and Schuette, Evan H.:
    Principles of Moment Distribution Applied to Stability of Structures
    Composed of Bars or Plates. NACA Rep. 809, 1945. (Supersedes NACA
    WR L-326.)

41. Stowell, Elbridge Z., and Lundquist, Eugene E.: Local Instability
    of Columns With I-, Z-, Channel, and Rectangular-Tube Sections.
    NACA TN 743, 1939.

42. Gerard, George: Critical Shear Stress of Plates Above the Propor-
    tional Limit. Jour. Appl. Mech., vol. 15, no. 1, Mar. 1948,
    pp. 7-12.

43. Stowell, Elbridge Z.: Critical Shear Stress of an Infinitely Long
    Plate in the Plastic Region. NACA TN 1681, 1948.

44. Lundquist, Eugene E., Schuette, Evan H., Heimerl, George J., and Roy,
    J. Albert: Column and Plate Compressive Strengths of Aircraft
    Structural Materials. 24S-T Aluminium-Alloy Sheet. NACA WR L-190,
    1945. (Formerly NACA ARR L5F01.)

45. Heimerl, George J., and Niles, Donald E.: Column and Plate Compres-
    sive Strengths of Aircraft Structural Materials. Extruded O-1HTA
    Magnesium Alloy. NACA TN 1156, 1947.

46. Bijlaard, P. P., and Wiseman, H. A. B.: On Theories of Plasticity
    and the Plastic Stability of Cruciform Sections. Jour. Aero. Sci.,
    vol. 20, Nov. 1953, p. 787.

47. Heimerl, George J.: Methods of Constructing Charts for Adjusting
    Test Results for the Compressive Strength of Plates for Differences
    in Material Properties. NACA TN 1564, 1948.

48. Pai, C. Hu, Lundquist, E. E., and Batdorf, S. B.: Effect of Small
    Deviations From Flatness on Effective Width and Buckling of Plates
    in Compression. NACA TN 1124, 1946.

TABLE 3.1.

COMPARISON OF THE DIFFERENTIAL QUOTIENT $d\gamma/d\tau$ BY INCREMENTAL

THEORY (F) AND DEFORMATION THEORY (D) OF MATERIAL UNDER

INITIAL COMPRESSIVE STRESS σ_0 IN THE PLASTIC RANGE

$E_t = 0.8E$			
τ	$E\left(\dfrac{d\gamma}{d\tau}\right)_F$	$E\left(\dfrac{d\gamma}{d\tau}\right)_D$	
		$E_{sec}(\sigma_0) = E$	$E_{sec}(\sigma_0) = 0.9E$
0	2.600	2.600	2.933
$.001\sigma_0$	2.600	2.600	2.933
$.003\sigma_0$	2.600	2.600	2.933
$.01\sigma_0$	2.600	2.600	2.933
$.03\sigma_0$	2.602	2.603	2.935
$.1\sigma_0$	2.622	2.632	2.951
$.3\sigma_0$	2.759	2.826	3.059

TABLE 3.2.

COMPARISON OF THE DIFFERENTIAL QUOTIENT $d\gamma/d\tau$ BY INCREMENTAL

THEORY (F) AND DEFORMATION THEORY (D) OF MATERIAL UNDER

INITIAL COMPRESSIVE STRESS σ_0 IN THE PLASTIC RANGE

$E_t = 0.6E$			
τ	$E\left(\dfrac{d\gamma}{d\tau}\right)_F$	$E\left(\dfrac{d\gamma}{d\tau}\right)_D$	
		$E_{sec}(\sigma_0) = E$	$E_{sec}(\sigma_0) = 0.9E$
0	2.600	2.600	2.933
$.001\sigma_0$	2.600	2.600	2.933
$.003\sigma_0$	2.600	2.600	2.933
$.01\sigma_0$	2.601	2.601	2.934
$.03\sigma_0$	2.605	2.608	2.940
$.1\sigma_0$	2.658	2.687	3.005
$.3\sigma_0$	3.025	3.203	3.435

TABLE 3.3.

COMPARISON OF THE DIFFERENTIAL QUOTIENT $d\gamma/d\tau$ BY INCREMENTAL

THEORY (F) AND DEFORMATION THEORY (D) OF MATERIAL UNDER

INITIAL COMPRESSIVE STRESS σ_0 IN THE PLASTIC RANGE

$E_t = 0.4E$				
τ	$E\left(\dfrac{d\gamma}{d\tau}\right)_F$	$E\left(\dfrac{d\gamma}{d\tau}\right)_D$		
		$E_{sec}(\sigma_0) = E$	$E_{sec}(\sigma_0) = 0.9E$	$E_{sec}(\sigma_0) = 0.5E$
0	2.600	2.600	2.933	5.600
$.001\sigma_0$	2.600	2.600	2.933	5.600
$.003\sigma_0$	2.600	2.600	2.933	5.600
$.01\sigma_0$	2.601	2.602	2.935	5.601
$.03\sigma_0$	2.612	2.618	2.950	5.606
$.1\sigma_0$	2.731	2.795	3.114	5.665
$.3\sigma_0$	3.557	3.956	4.189	6.052

TABLE 3.4.

COMPARISON OF THE DIFFERENTIAL QUOTIENT $d\gamma/d\tau$ BY INCREMENTAL

THEORY (F) AND DEFORMATION THEORY (D) OF MATERIAL UNDER

INITIAL COMPRESSIVE STRESS σ_0 IN THE PLASTIC RANGE

$E_t = 0.2E$				
τ	$E\left(\dfrac{d\gamma}{d\tau}\right)_F$	$E\left(\dfrac{d\gamma}{d\tau}\right)_D$		
		$E_{sec}(\sigma_0) = E$	$E_{sec}(\sigma_0) = 0.9E$	$E_{sec}(\sigma_0) = 0.5E$
0	2.600	2.600	2.933	5.600
$.001\sigma_0$	2.600	2.600	2.933	5.600
$.003\sigma_0$	2.600	2.600	2.933	5.600
$.01\sigma_0$	2.604	2.605	2.938	5.604
$.03\sigma_0$	2.632	2.648	2.980	5.636
$.1\sigma_0$	2.949	3.120	3.439	5.990
$.3\sigma_0$	5.151	6.216	6.448	8.312

TABLE 3.5.

COMPARISON OF THE DIFFERENTIAL QUOTIENT $d\gamma/d\tau$ BY INCREMENTAL THEORY (F) AND

DEFORMATION THEORY (D) OF MATERIAL UNDER INITIAL COMPRESSIVE

STRESS σ_0 IN THE PLASTIC RANGE

		$E_t = 0.1E$			
τ	$E\left(\dfrac{d\gamma}{d\tau}\right)_F$	$E\left(\dfrac{d\gamma}{d\tau}\right)_D$			
		$E_{sec}(\sigma_0) = E$	$E_{sec}(\sigma_0) = 0.9E$	$E_{sec}(\sigma_0) = 0.5E$	$E_{sec}(\sigma_0) = 0.15E$
0	2.600	2.600	2.933	5.600	19.600
$.001\sigma_0$	2.600	2.600	2.933	5.600	19.600
$.003\sigma_0$	2.602	2.600	2.933	5.600	19.600
$.01\sigma_0$	2.608	2.611	2.944	5.610	19.604
$.03\sigma_0$	2.673	2.708	3.040	5.696	19.640
$.1\sigma_0$	3.386	3.770	4.089	6.640	20.033
$.3\sigma_0$	8.340	10.735	10.968	12.831	22.613

TABLE 3.6.

COMPARISON OF THE DIFFERENTIAL QUOTIENT $d\gamma/d\tau$ BY INCREMENTAL THEORY (F) AND

DEFORMATION THEORY (D) OF MATERIAL UNDER INITIAL COMPRESSIVE

STRESS σ_0 IN THE PLASTIC RANGE

$E_t = 0.05E$					
τ	$E\left(\dfrac{d\gamma}{d\tau}\right)_F$	$E\left(\dfrac{d\gamma}{d\tau}\right)_D$			
		$E_{sec}(\sigma_0) = E$	$E_{sec}(\sigma_0) = 0.9E$	$E_{sec}(\sigma_0) = 0.5E$	$E_{sec}(\sigma_0) = 0.15E$
0	2.600	2.600	2.933	5.600	19.601
$.001\sigma_0$	2.600	2.600	2.933	5.600	19.601
$.003\sigma_0$	2.601	2.600	2.933	5.600	19.601
$.01\sigma_0$	2.617	2.623	2.956	5.622	19.617
$.03\sigma_0$	2.753	2.828	3.160	5.816	19.761
$.1\sigma_0$	4.260	5.070	5.389	7.940	21.334
$.3\sigma_0$	14.718	19.774	20.007	21.870	31.653

TABLE 3.7.

COMPARISON OF THE DIFFERENTIAL QUOTIENT $d\gamma/d\tau$ BY INCREMENTAL THEORY (F) AND

DEFORMATION THEORY (D) OF MATERIAL UNDER INITIAL COMPRESSIVE

STRESS σ_0 IN THE PLASTIC RANGE

τ	$E\left(\frac{d\gamma}{d\tau}\right)_F$	$E\left(\frac{d\gamma}{d\tau}\right)_D$			
		$E_{sec}(\sigma_0) = E$	$E_{sec}(\sigma_0) = 0.9E$	$E_{sec}(\sigma_0) = 0.5E$	$E_{sec}(\sigma_0) = 0.15E$
0	2.600	2.600	2.933	5.600	19.601
$.001\sigma_0$	2.600	2.600	2.933	5.600	19.601
$.003\sigma_0$	2.604	2.600	2.933	5.600	19.601
$.01\sigma_0$	2.644	2.659	2.992	5.658	19.653
$.03\sigma_0$	2.996	3.188	3.520	6.176	20.121
$.1\sigma_0$	6.882	8.970	9.289	11.840	25.234
$.3\sigma_0$	33.891	46.891	47.124	48.987	58.770

$E_t = 0.02E$ (header spanning entire table)

TABLE 3.8.

COMPARISON OF THE DIFFERENTIAL QUOTIENT $d\gamma/d\tau$ BY INCREMENTAL THEORY (F) AND

DEFORMATION THEORY (D) OF MATERIAL UNDER INITIAL COMPRESSIVE

STRESS σ_0 IN THE PLASTIC RANGE

$E_t = 0.01E$					
τ	$E\left(\dfrac{d\gamma}{d\tau}\right)_F$	$E\left(\dfrac{d\gamma}{d\tau}\right)_D$			
		$E_{sec}(\sigma_0) = E$	$E_{sec}(\sigma_0) = 0.9E$	$E_{sec}(\sigma_0) = 0.5E$	$E_{sec}(\sigma_0) = 0.15E$
0	2.600	2.600	2.933	5.600	19.601
$.001\sigma_0$	2.601	2.600	2.933	5.600	19.601
$.003\sigma_0$	2.608	2.600	2.933	5.600	19.601
$.01\sigma_0$	2.689	2.719	3.052	5.718	19.713
$.03\sigma_0$	3.400	3.788	4.120	6.776	20.721
$.1\sigma_0$	11.251	15.470	15.789	18.340	31.734
$.3\sigma_0$	65.742	92.086	92.319	94.182	103.96

TABLE 3.9.

RESULTS OF ONAT AND DRUCKER BUCKLING CASE

		Initial torsion per length 2b of section in radians	0	0.000111	0.00111	0.0111
Incremental theory		$\bar{\sigma} = \sigma_{max}, \sigma*$ is elastic limit	$2\sigma*$	$1.26\sigma*$	$1.17\sigma*$	$1.08\sigma*$
		Torsion per length 2b at maximum load in radians	0	0.060	0.067	0.077
		τ/σ at maximum load	0	0.100	0.112	0.128
Deformation theory		$\bar{\sigma} = \sigma_{max}, \sigma*$ is elastic limit	$1.05\sigma*$			$1.02\sigma*$
		Torsion per length 2b at maximum load in radians	0			0.050
		τ/σ at maximum load	0			0.083
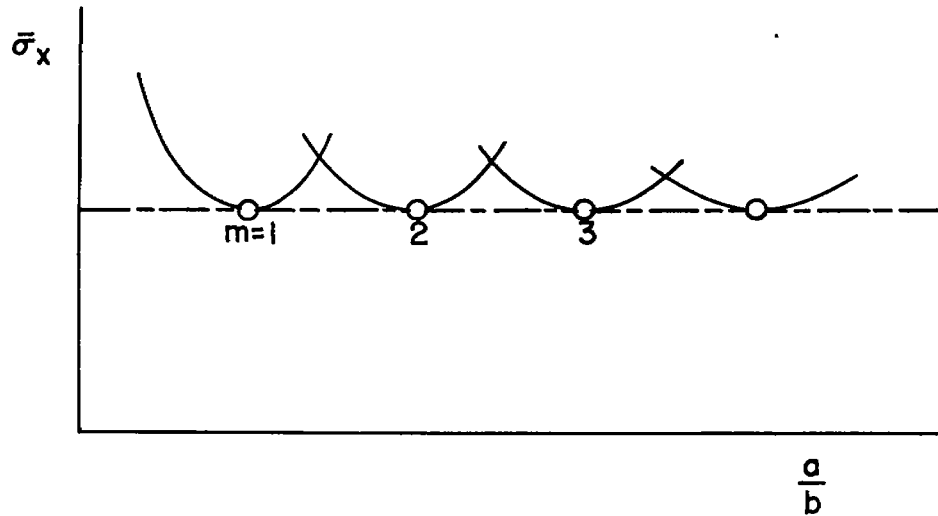
Figure 2.1.- Critical compressive stress $\bar{\sigma}_x$ of rectangular plate
   loaded under compression in one direction, all edges hinge
   supported; length of sides a and b; width-depth ratio (b/h) is
   constant. The sides of length b are the loaded sides.
   m = half-waves.

$\bar{\sigma}_x$

By elasticity theory

Elastic theory

$\lambda = \dfrac{b}{h}\sqrt{12(1-\nu^2)}$
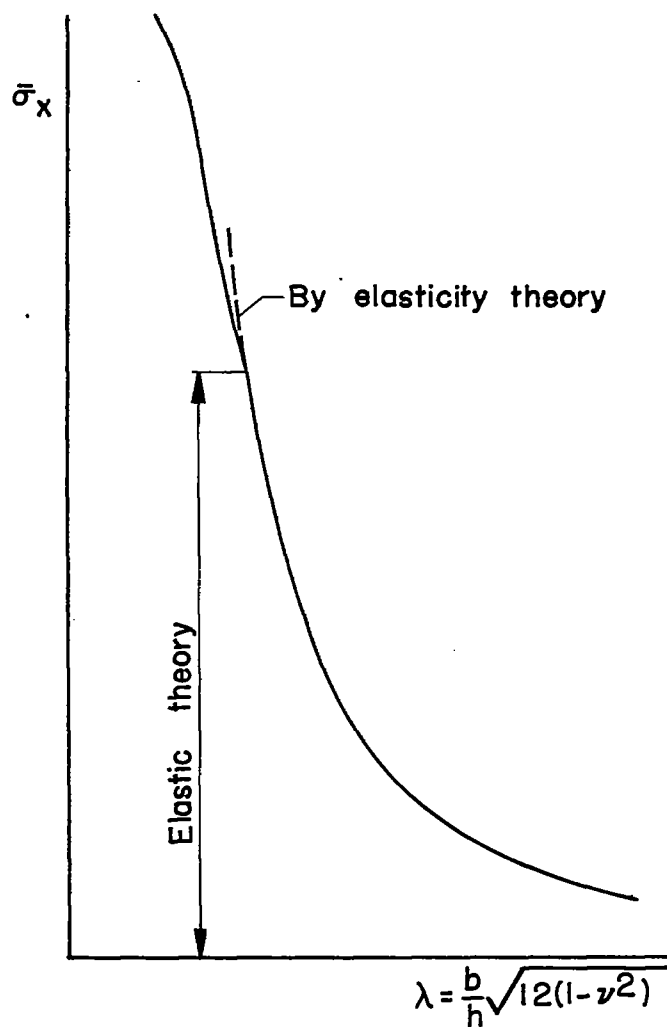
Figure 2.2- Method of plotting used by Kollbrunner. Critical compressive load $\bar{\sigma}_x$ of an infinitely long plate with hinged edges under compression in the direction of the length.
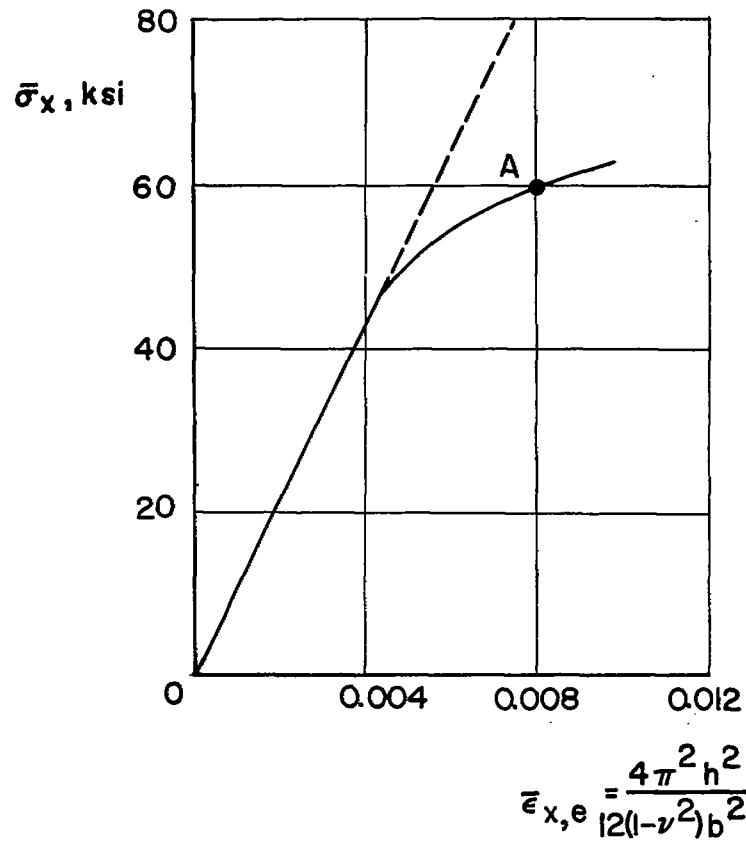
Figure 2.3.- NACA method No. 1. Vertical: critical stress $\bar{\sigma}_x$
of an infinitely long plate of 14S-T6 aluminum with hinged edges
under compression in length direction. Horizontal: critical
strain $\bar{\epsilon}_{x,e}$ by elasticity theory.

$$\eta = \frac{\sigma_x}{\bar{\sigma}_{x,e}} = \bar{\sigma}_x \frac{12(1-\nu^2)b^2}{4\pi^2 Eh^2}$$
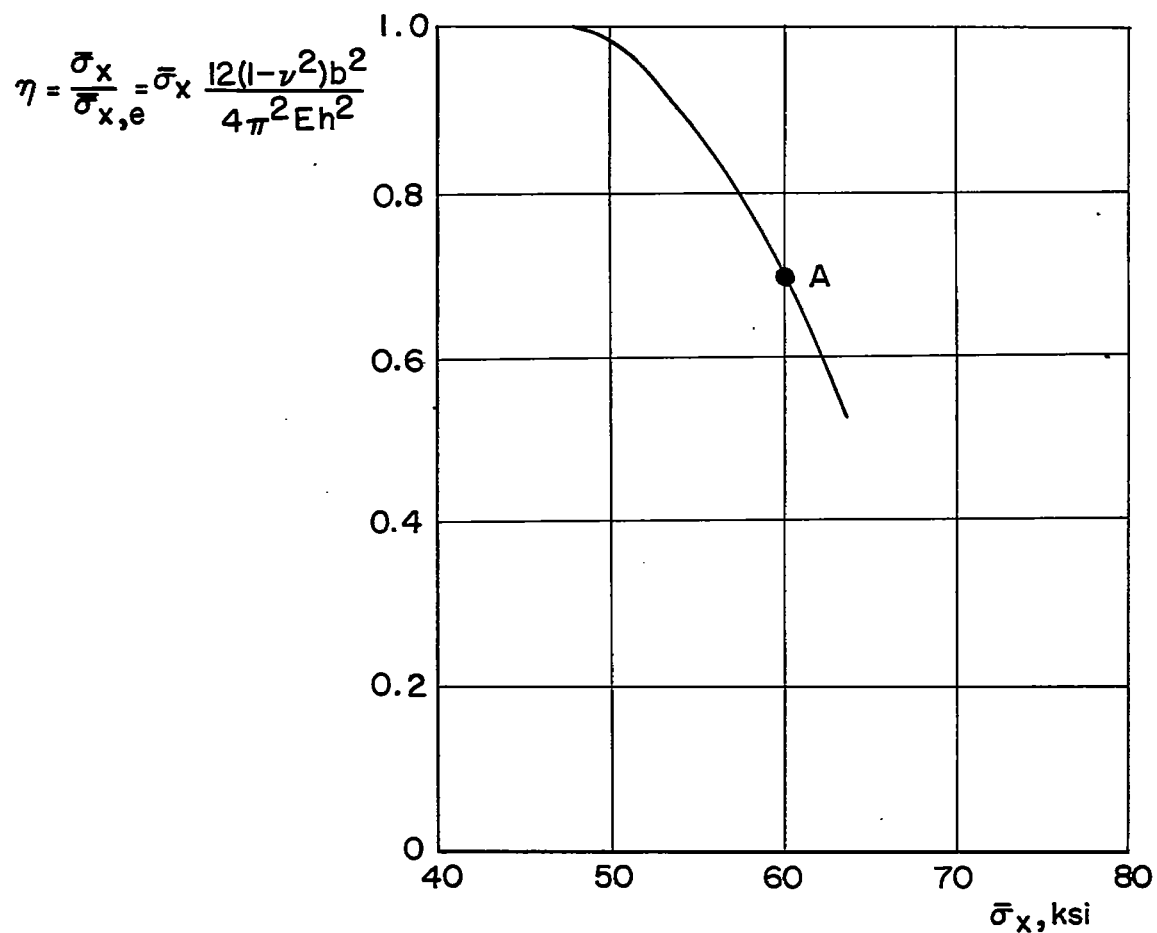
Figure 2.4.- NACA method No. 2. Load case as in figure 2.2. Vertical: factor η by which $\bar{\sigma}_{x,e}$ should be multiplied according to elasticity theory to yield actual critical stress $\bar{\sigma}_x$. Horizontal: actual stress $\bar{\sigma}_x$.
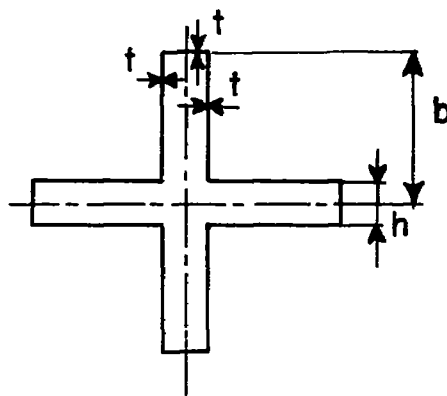
Figure 3.1.- Onat and Drucker cruciform.
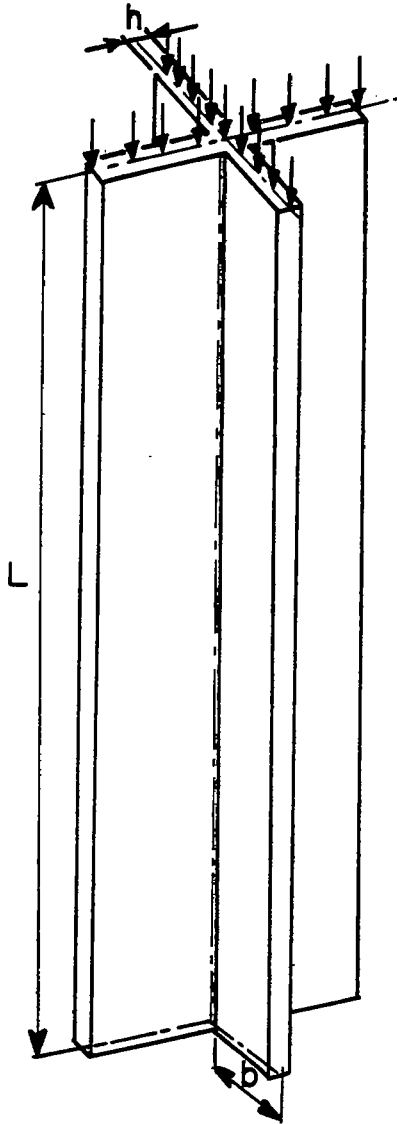
Figure 3.2.- Cruciform in straight state.
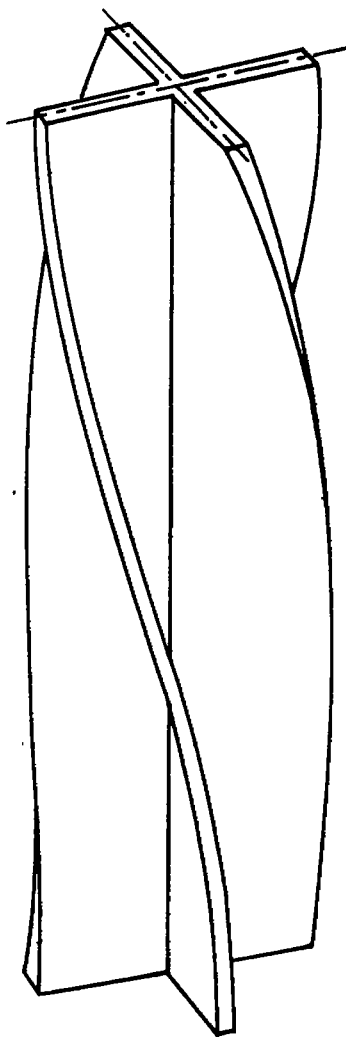
Figure 3.3-   Cruciform in twisted state.
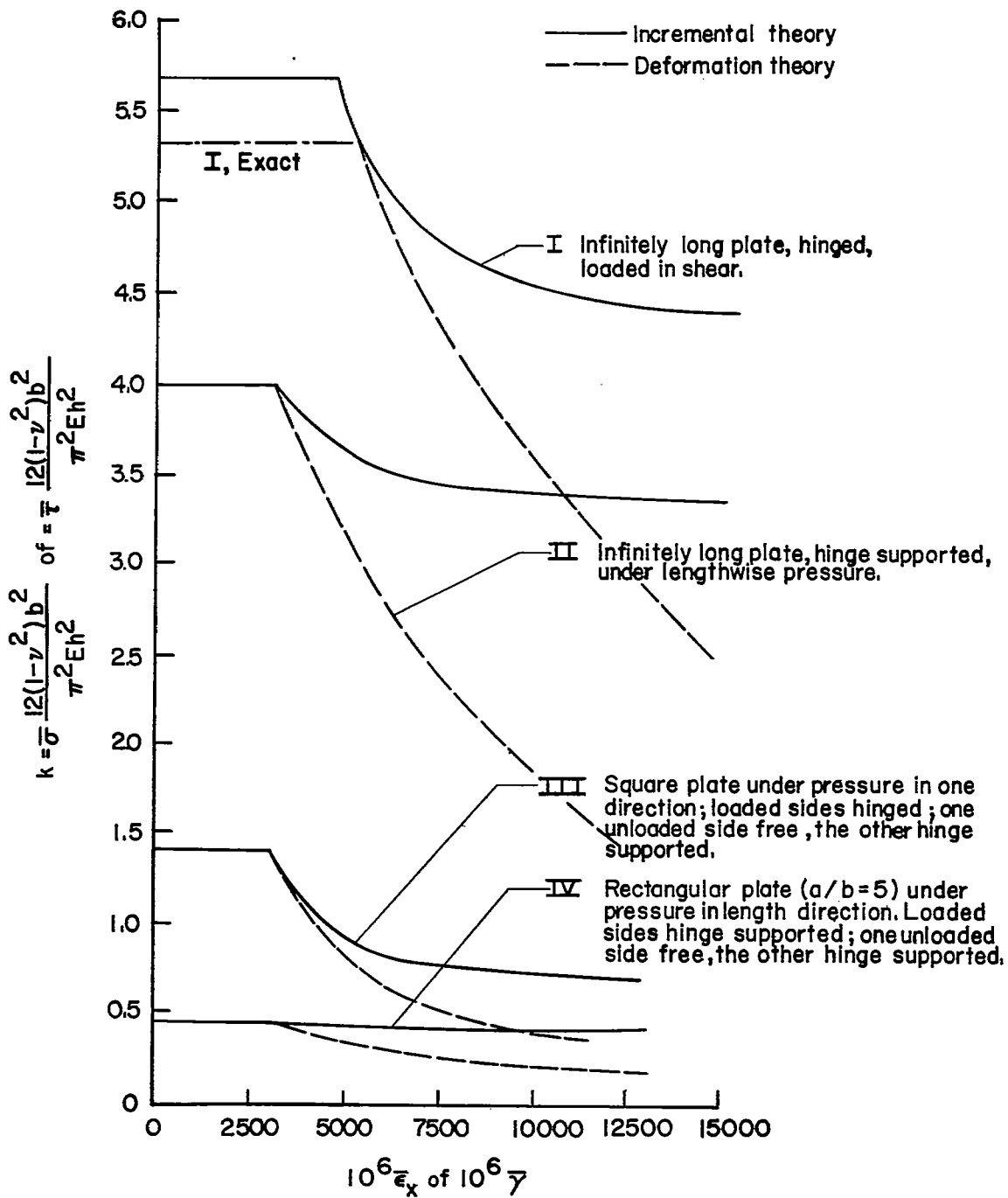
Figure 3.4- Buckling factor k plotted against $\bar{\epsilon}_x$ (or shear $\bar{\gamma}$) for four different cases of 24S-T aluminum, according to Besseling (ref. 1).

$$k = \bar{\sigma}_x \frac{12(1-\nu^2)b^2}{\pi^2 Eh^2}$$

$$\frac{b^2}{h^2} = 1000$$
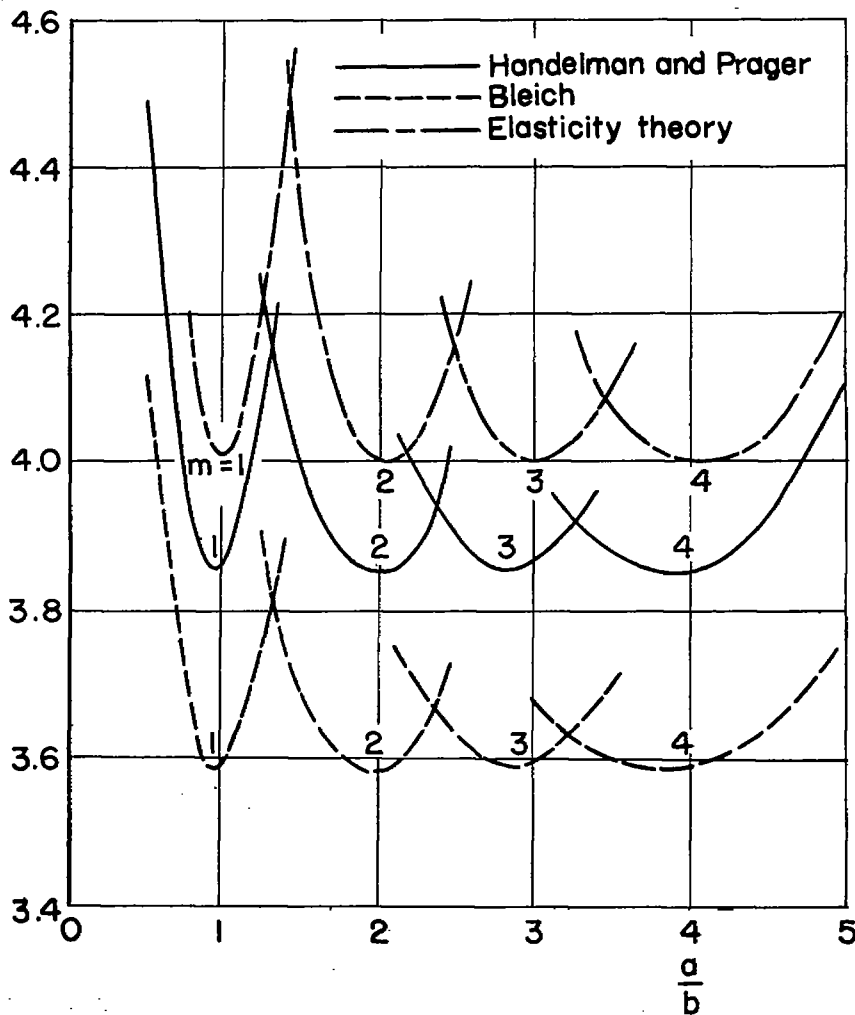
Figure 3.5.- Buckling factor k for simply supported rectangular plate ν = 0.32 hinge supported on all edges under compression. The sides of length b are loaded, width/thickness ratio according to $b^2/h^2 = 1000$. m = half-waves at buckling (taken from ref. 9).

$$k = \bar{\sigma}_x \, \frac{12(1-\nu^2)b^2}{\pi^2 E h^2}$$
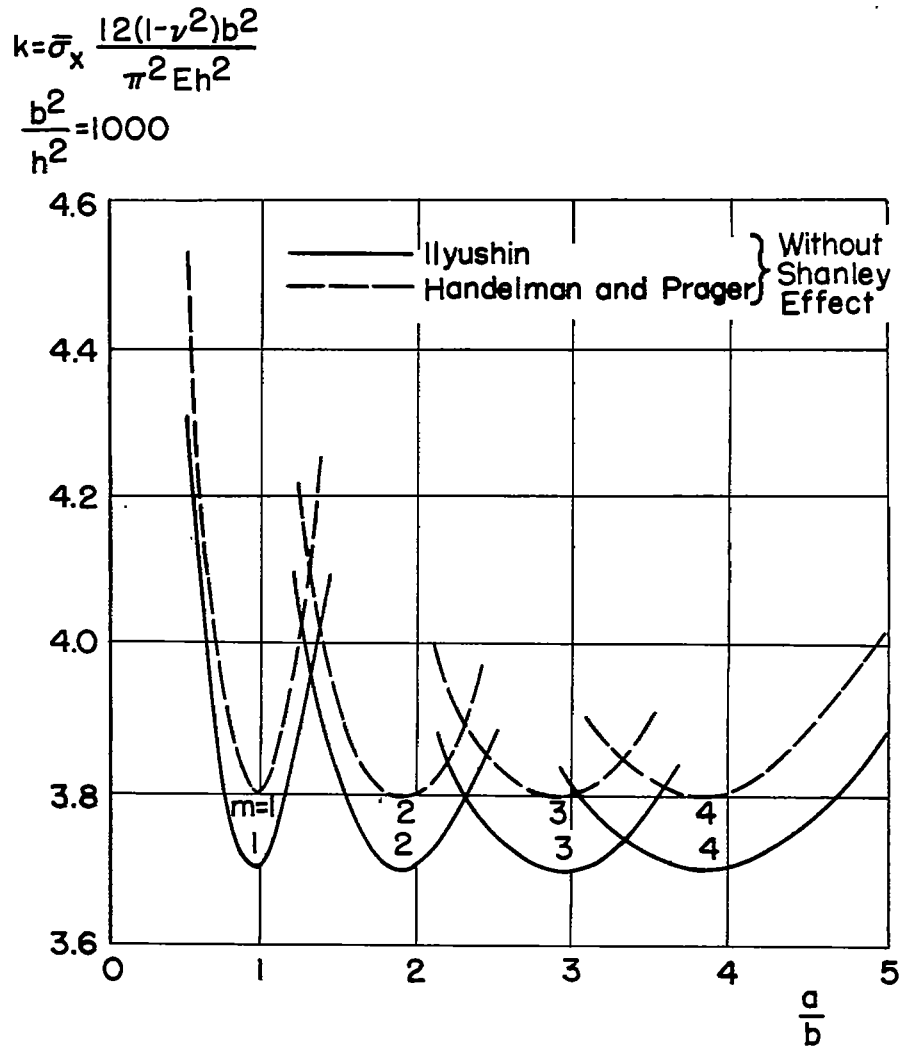
$$\frac{b^2}{h^2} = 1000$$

Figure 3.6.- Buckling factor k for simply supported rectangular plate $\nu = 0.50$, all edges hinge supported, loaded in compression. The sides of length b are loaded; width/thickness ratio according to $b^2/h^2 = 1000$. m = half-waves at buckling (taken from ref. 9).
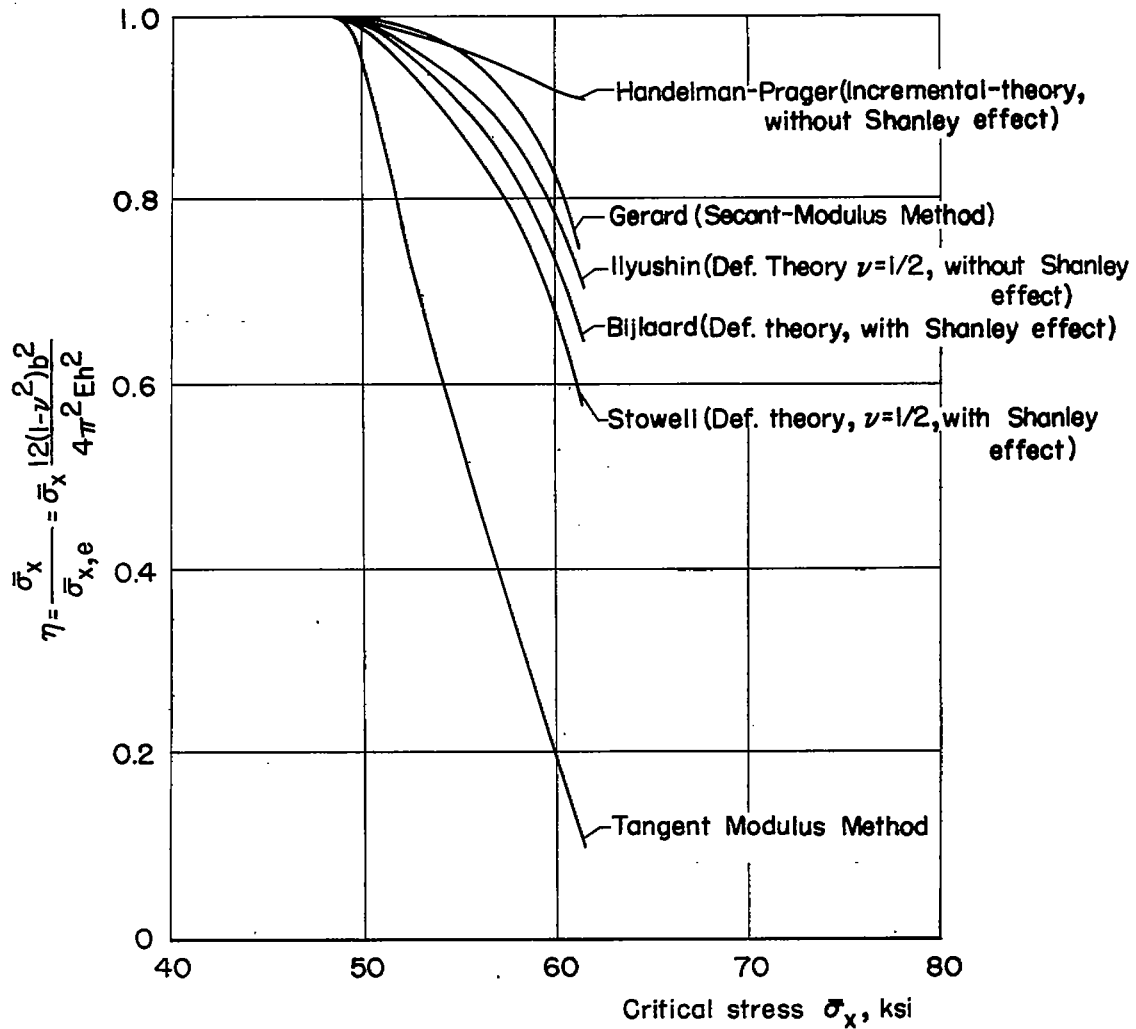
Figure 3.7.- Factor η plotted against critical stress $\bar{\sigma}_x$ for an infinitely long plate of 14S-T6 aluminum plate, with hinge-supported edges under compression in length direction (taken from ref. 30).
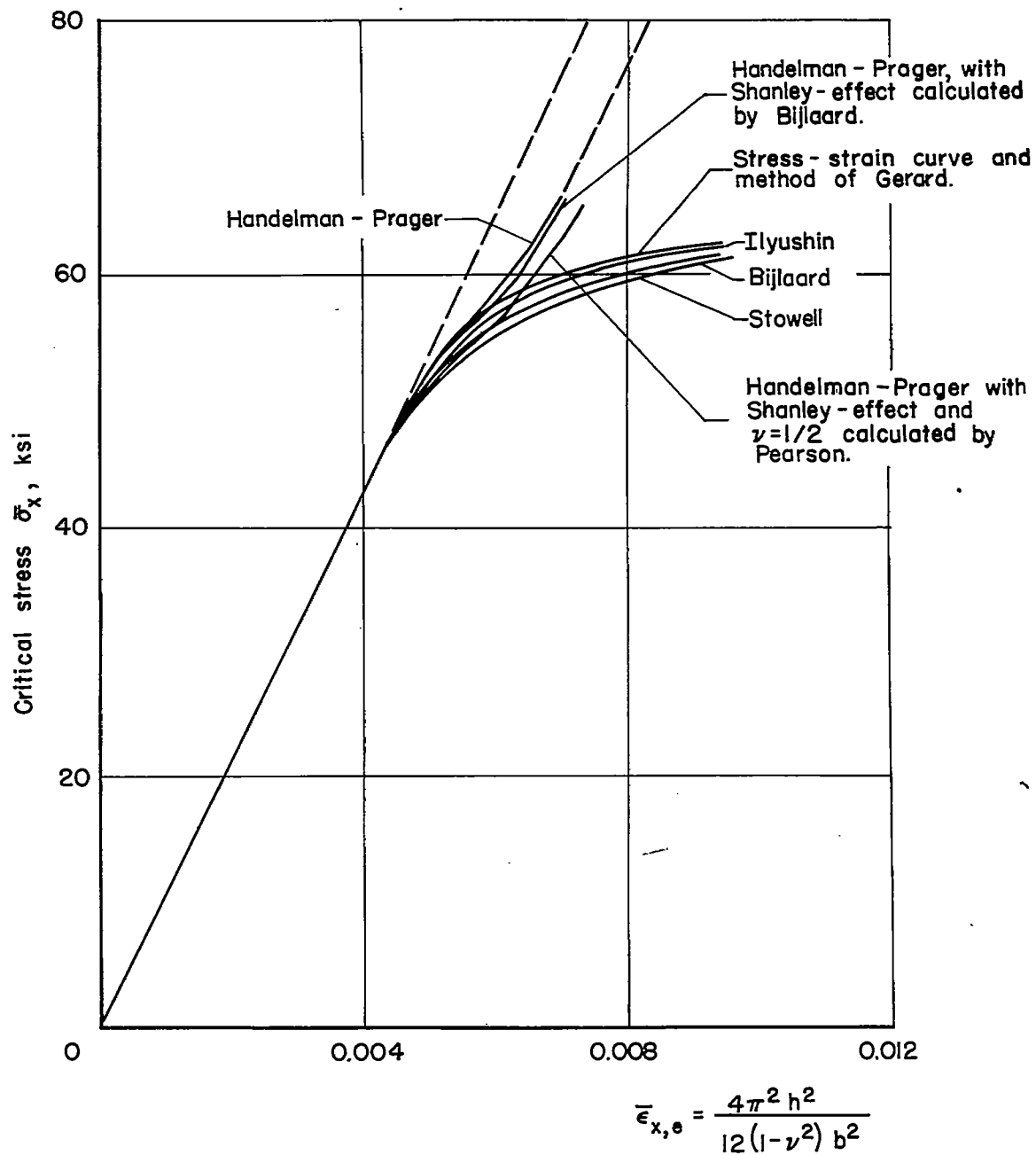
Figure 3.8.- Load case in figure 3.4. Critical stress $\bar{\sigma}_x$ plotted
against critical strain $\bar{\epsilon}_{x,e}$ computed by elasticity theory (taken
from refs. 30 and 31).
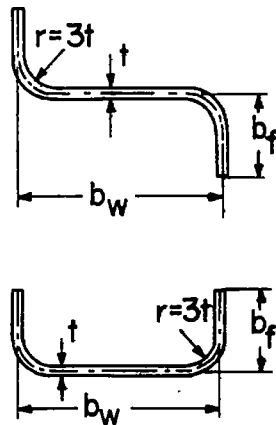
Figure 4.1.- Sections used in tests described in reference 32.
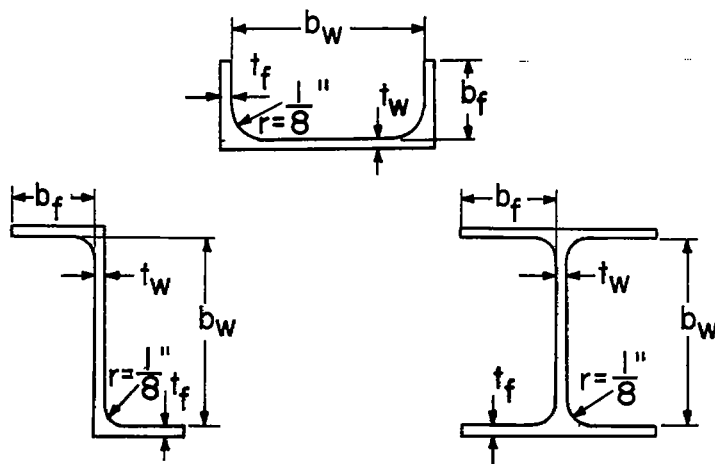
Figure 4.2.- Sections used in tests described in references 33 to 36.
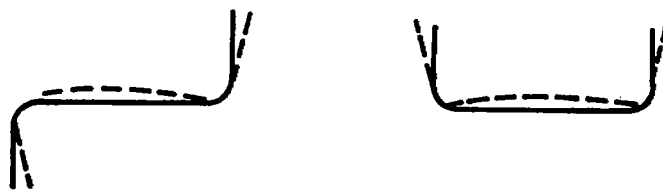
Figure 4.3.- Cross-sectional distortion during buckling in tests
described in reference 32.
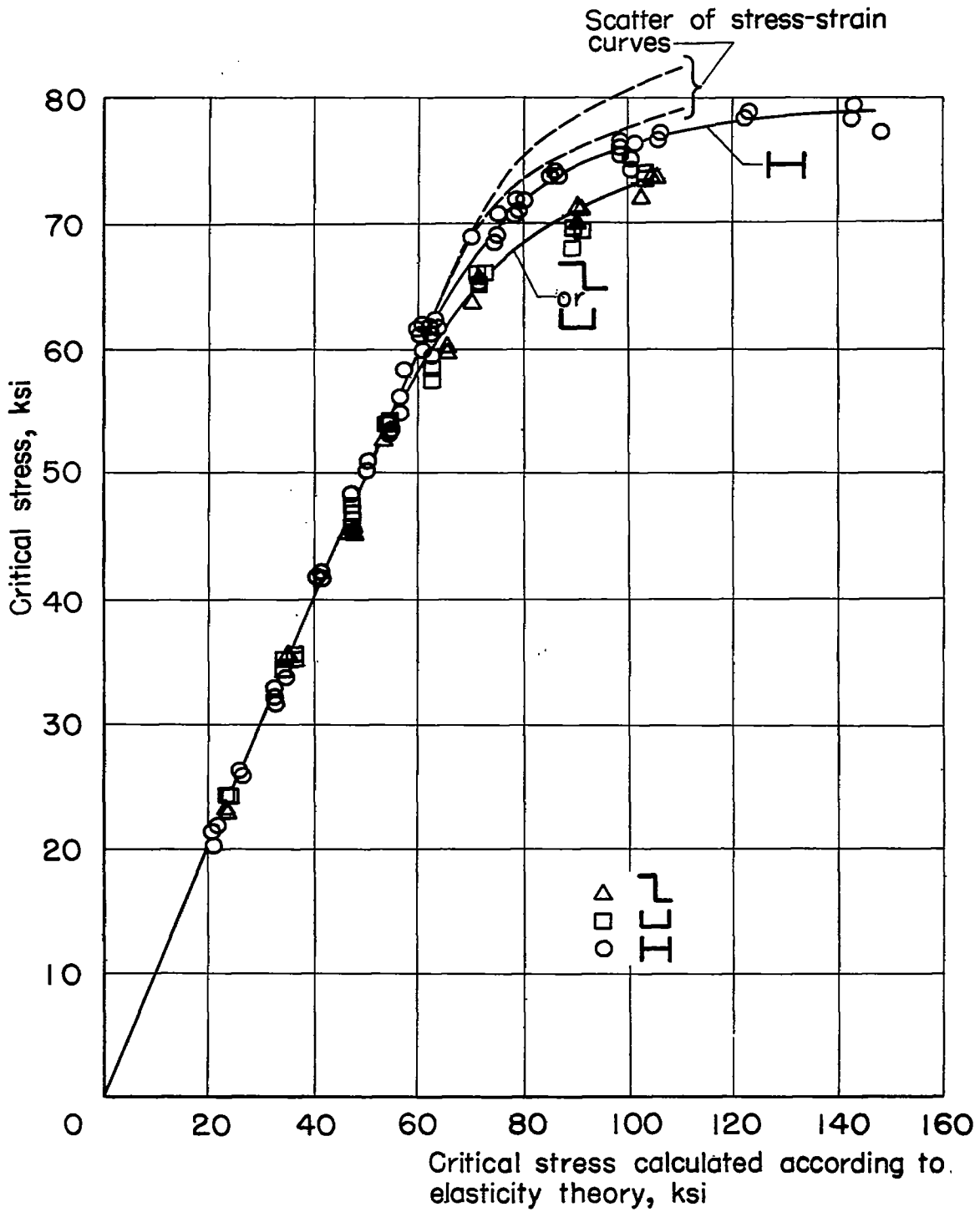
Figure 4.4.- Experimental results of compression tests on sections
described in reference 33; material, 75S-T aluminum.
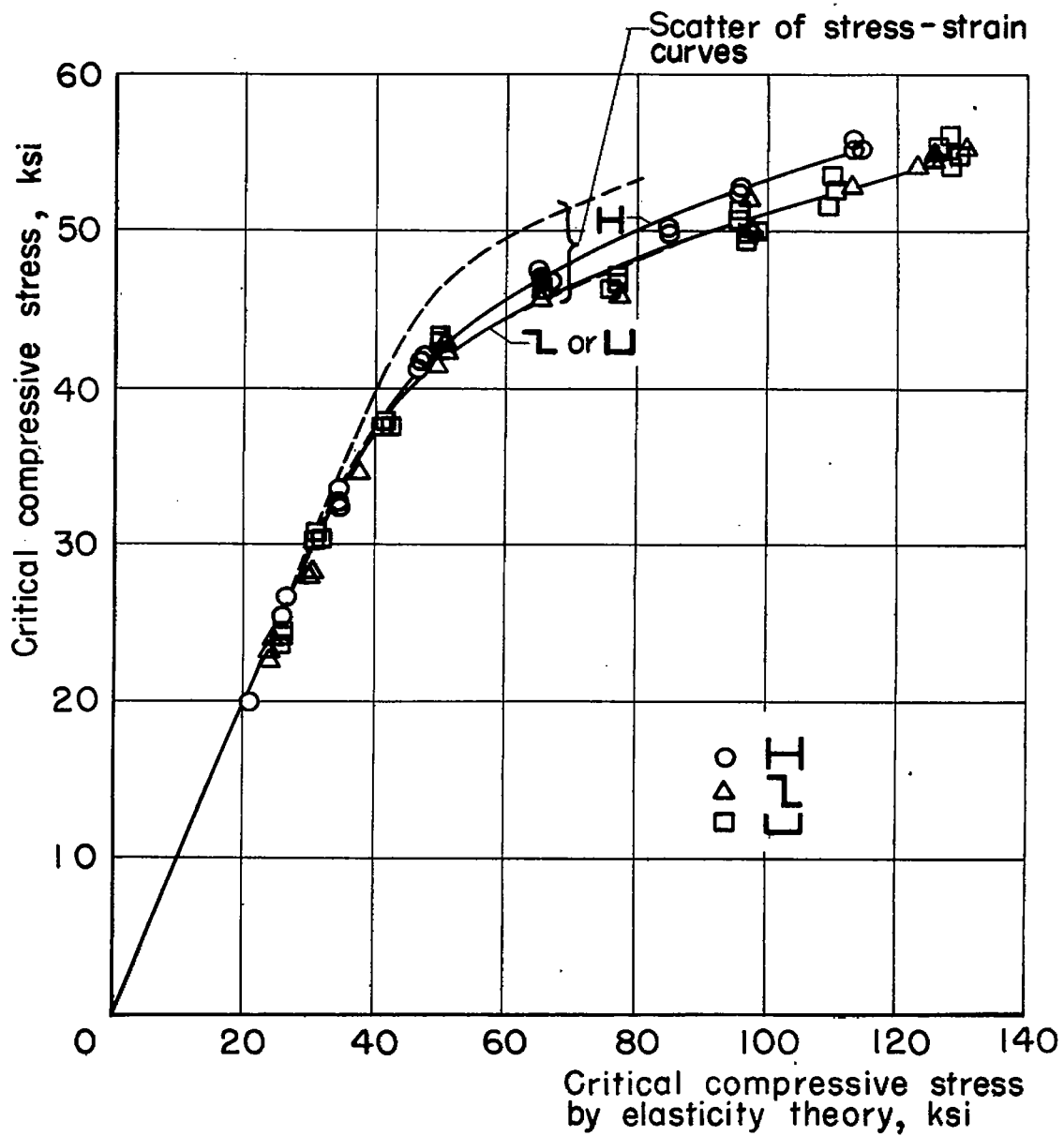
Figure 4.5.- Experimental results of compression tests on sections described in reference 34; material, 24S-T aluminum.
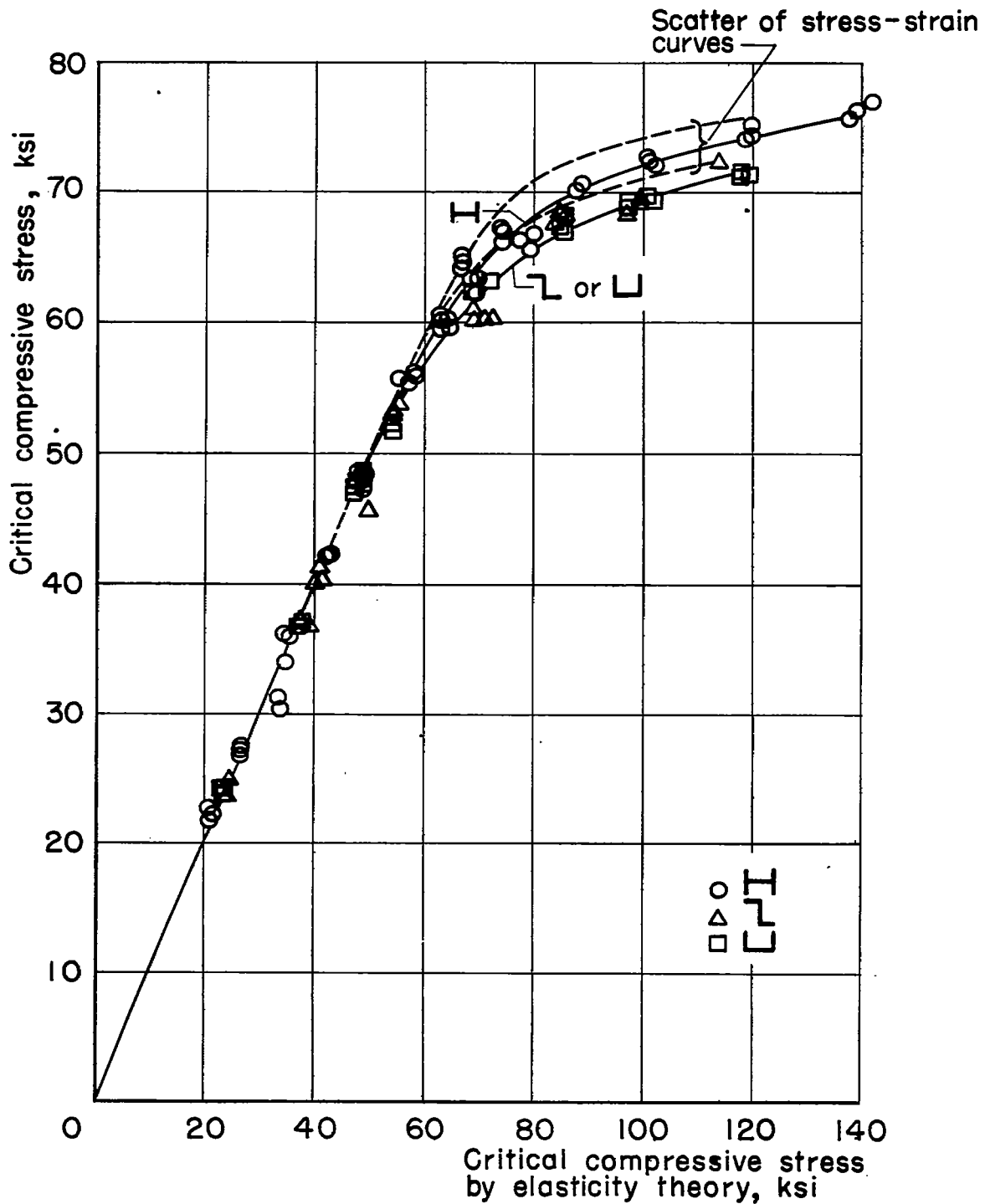
Figure 4.6.- Experimental results of compression tests on sections described in reference 35; material, R 303-T extruded aluminum.
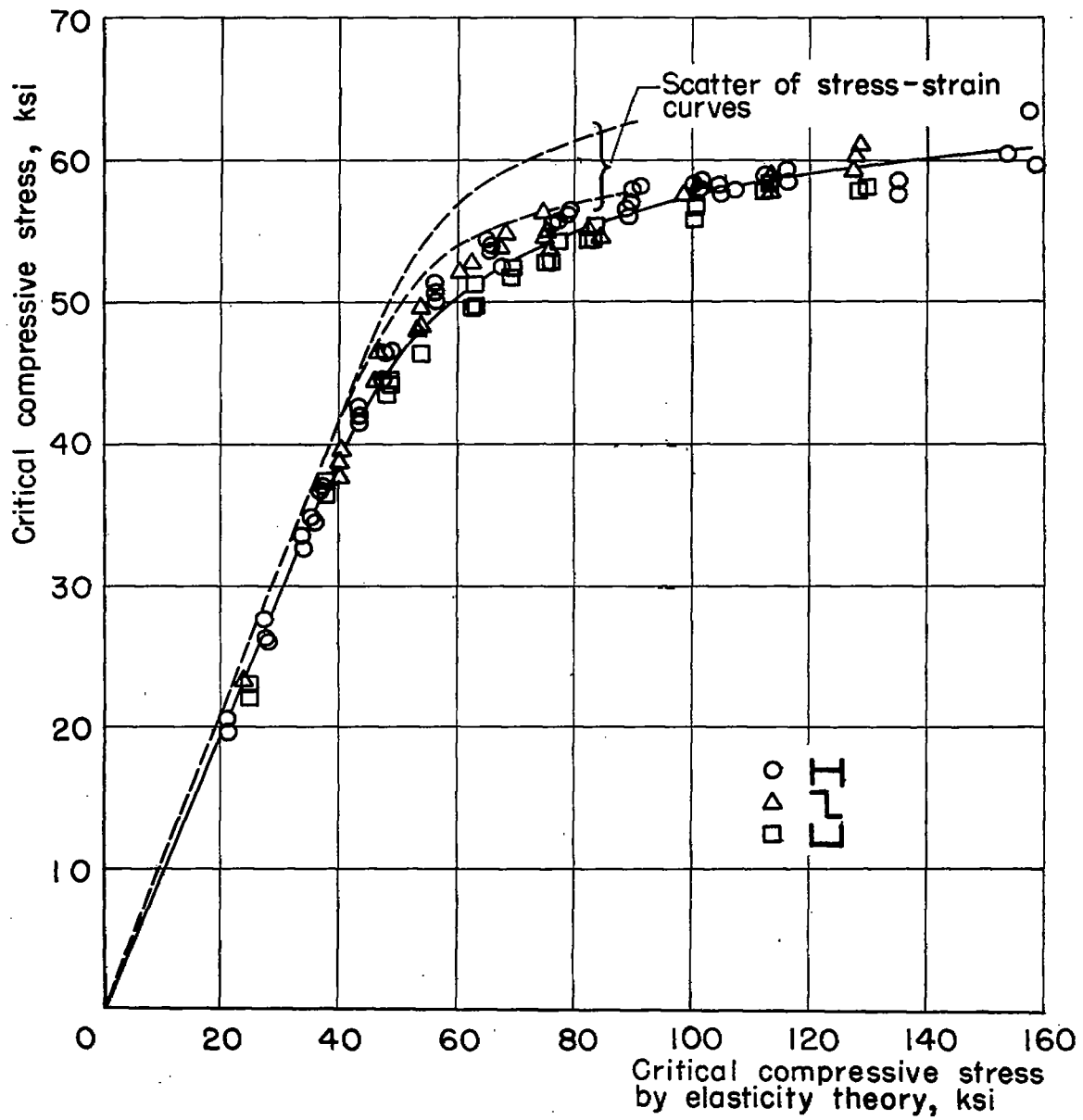
Figure 4.7.- Experimental results of compression tests on sections of 14S-T extruded aluminum (from ref. 36).
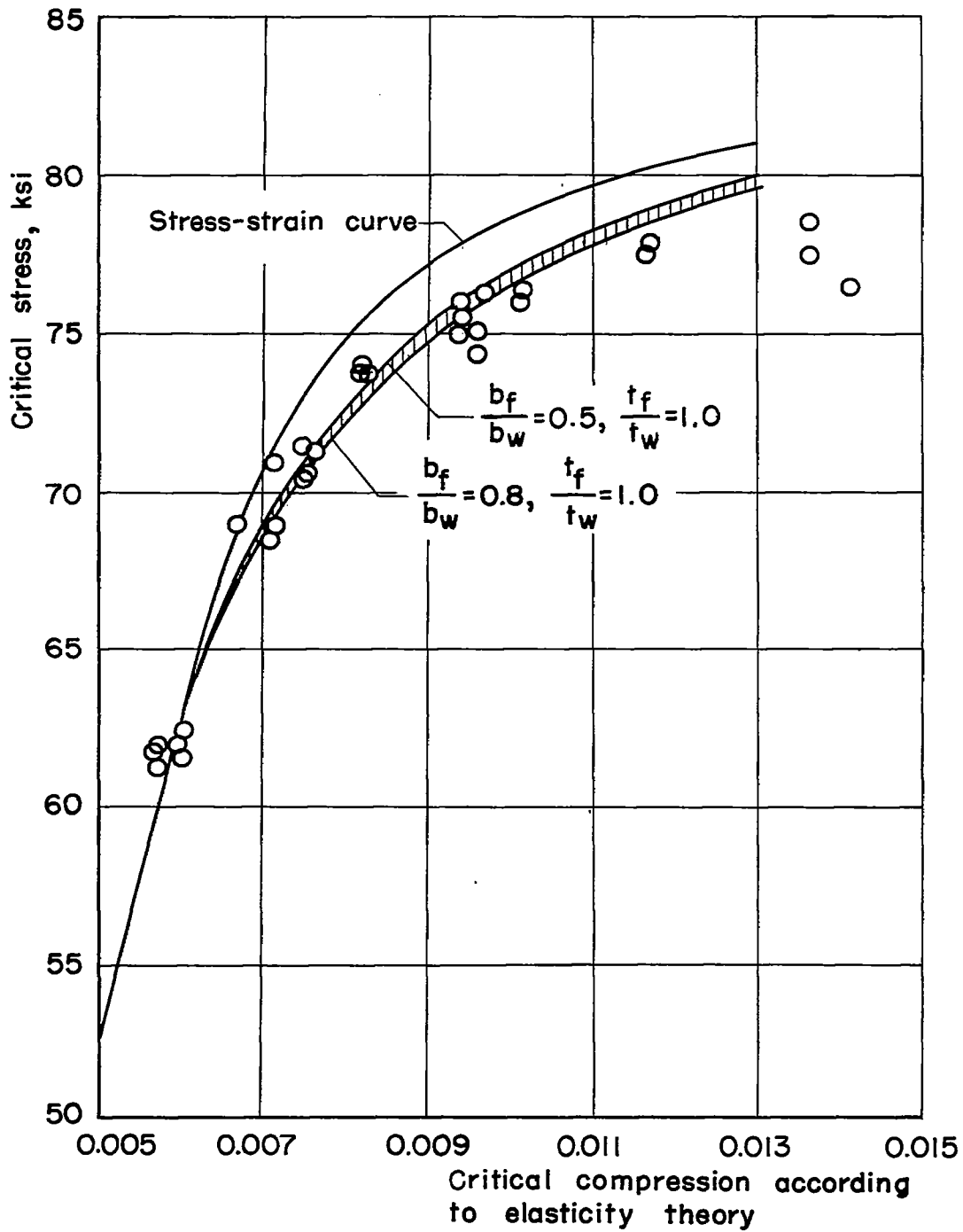
Figure 4.8.- Experimental results of compression tests of reference 31, as concerns H-sections; compared with theoretical results of Stowell (taken from ref. 38; for b_F, b_W, t_F, and t_W, see fig. 4.2).
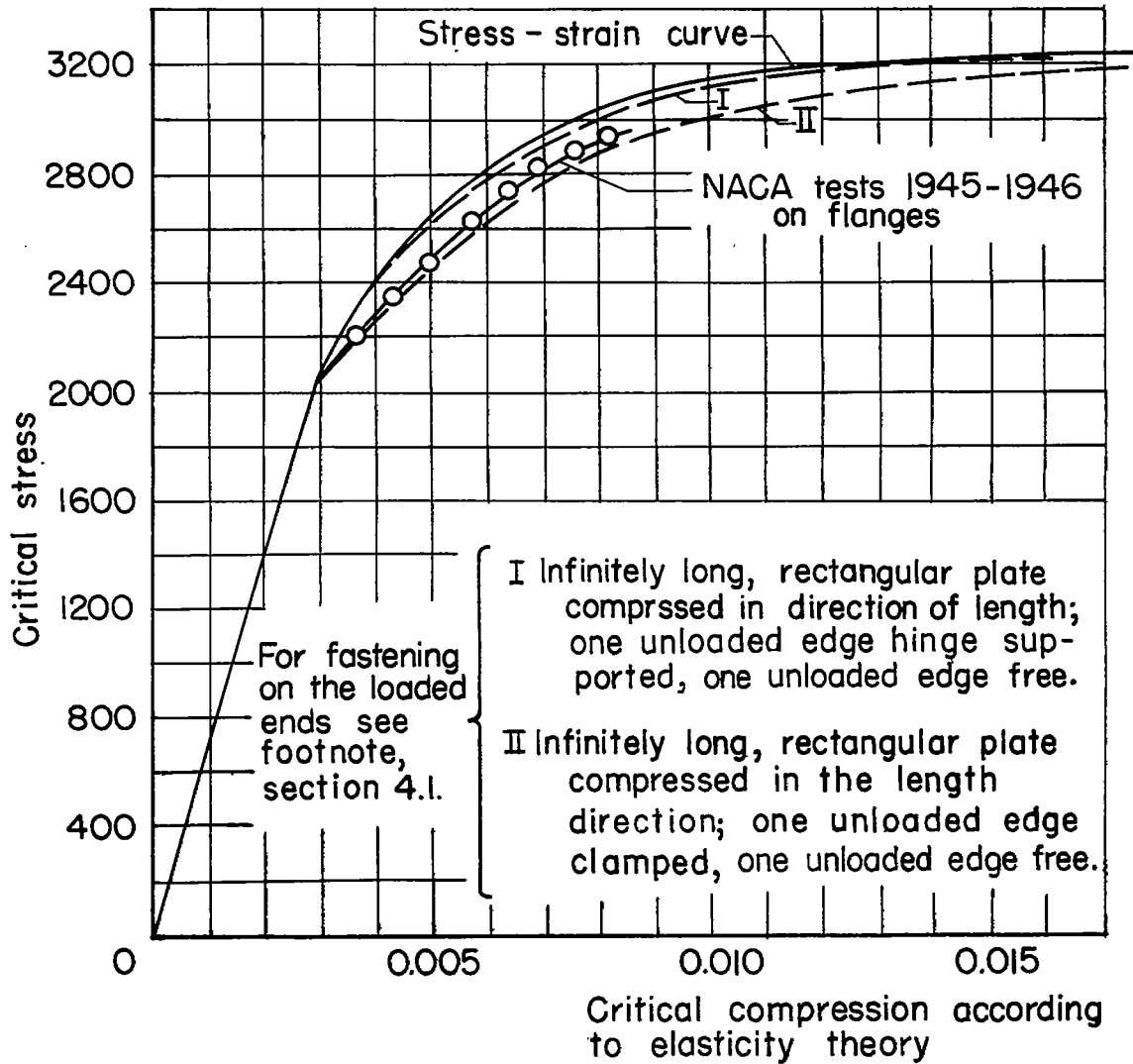
Figure 4.9.- Two buckling cases calculated by Bijlaard, compared with NACA test on sections (taken from ref. 22).
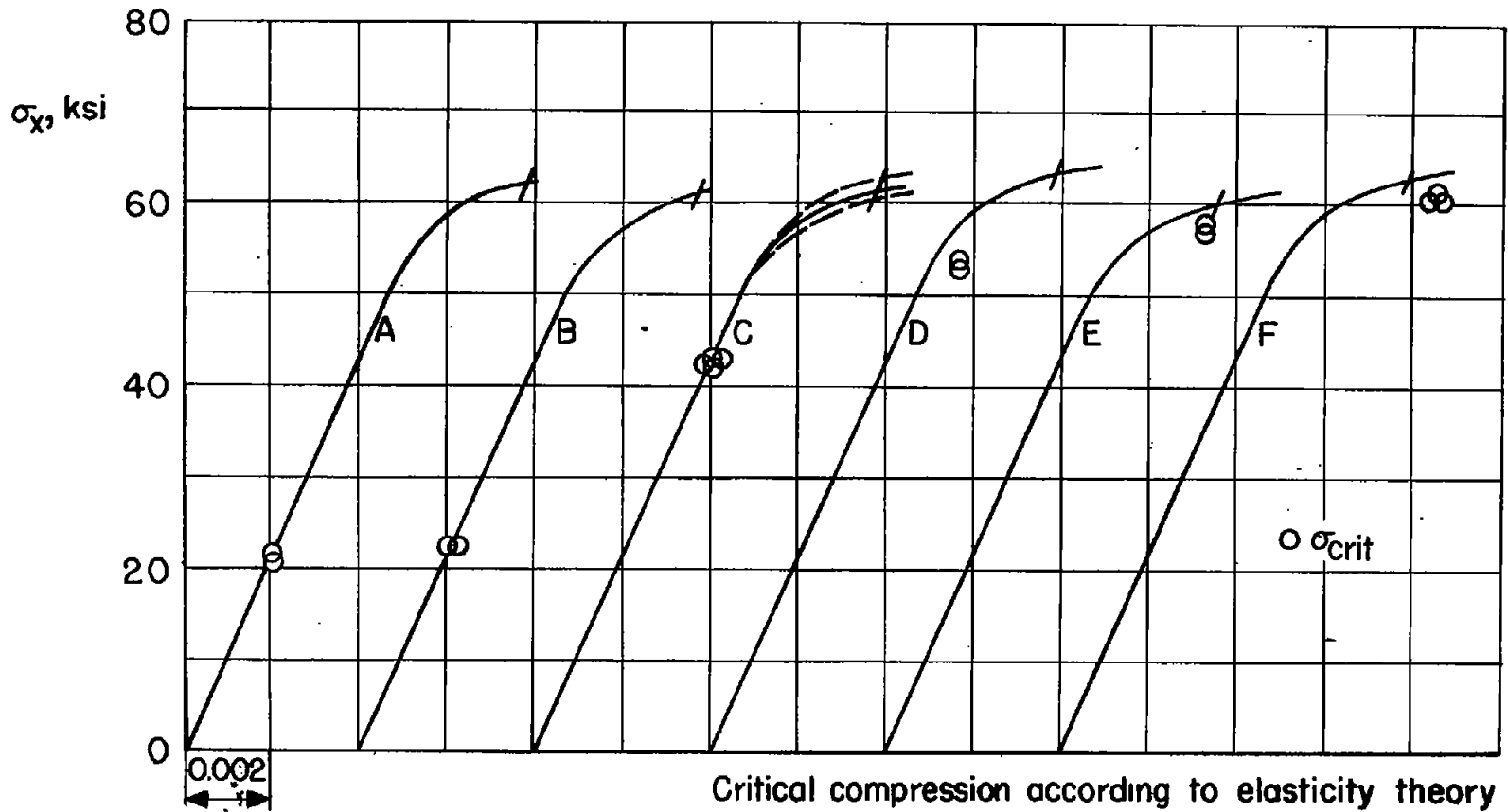
$$\bar{\epsilon}_{x,e} = \frac{4\pi^2 h^2}{12(1-\nu^2)b^2}$$

Figure 4.10.- Critical stress $\bar{\sigma}_x$ of infinitely long 14S-T aluminum alloy plate, hinge-supported edges, compressed in length direction. The seven curves refer to seven groups of test pieces, each group being manufactured from the same box-beam section. The curves are those of Gerard, hence stress-strain curves (from ref. 30).
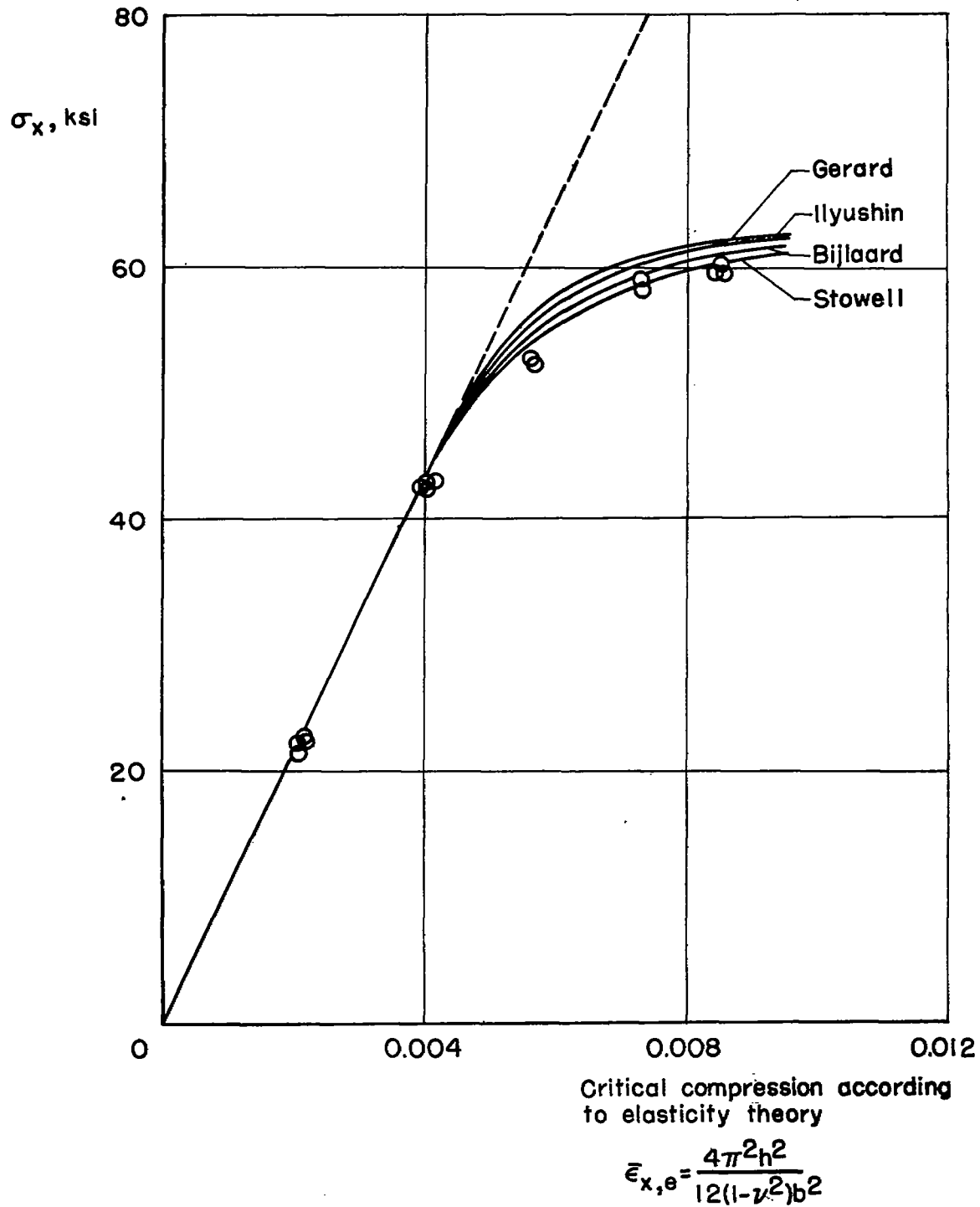
Figure 4.11.- Measurements of figure 4.10, corrected for material with constant stress-strain curve. The theoretical curves are those of figure 3.8 (taken from ref. 30).
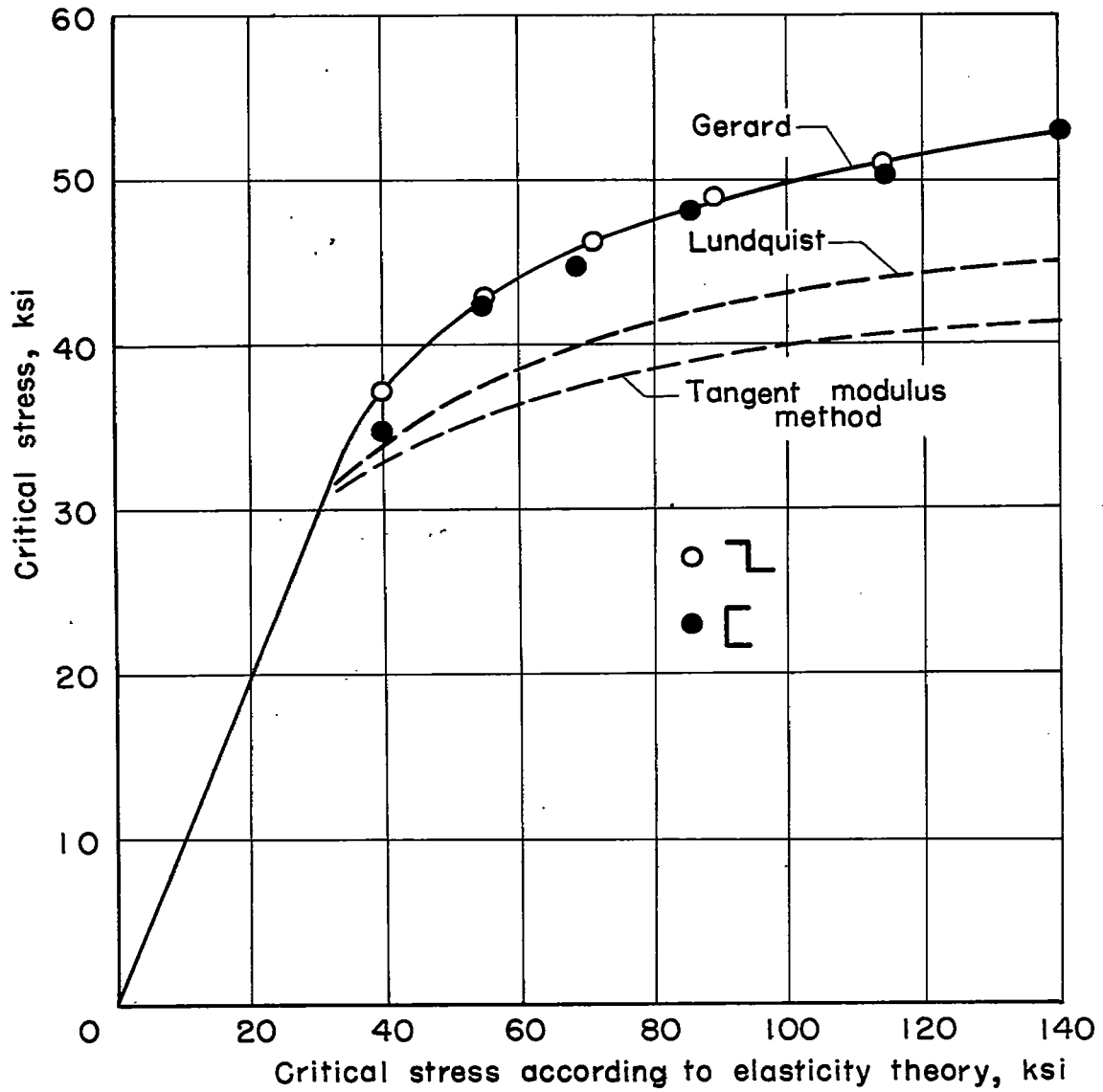
Figure 4.12.- Results of compression tests on 24S-T aluminum sections
by Gerard (taken from ref. 19).
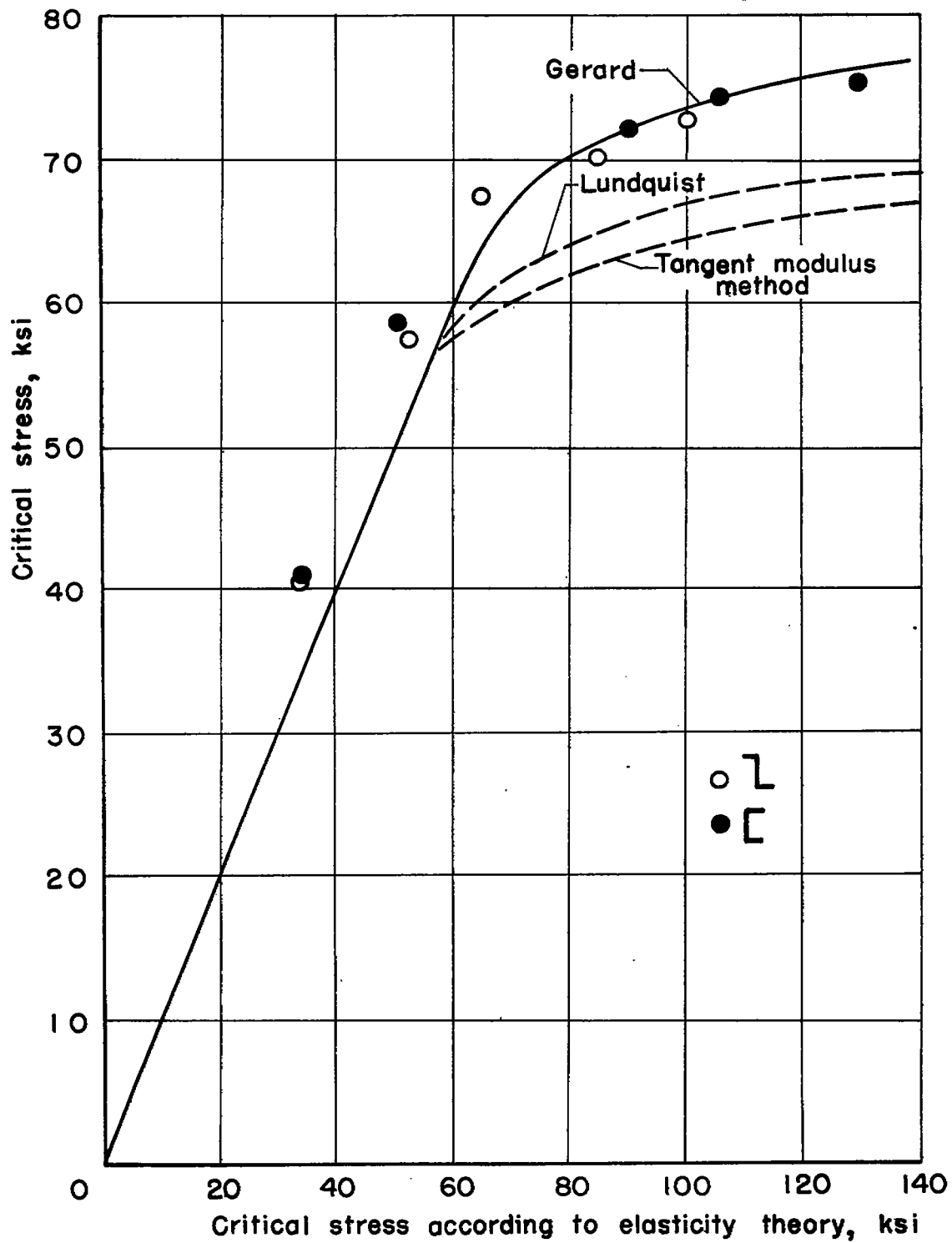
Figure 4.13.- Results of compression tests on sections of 75S-T
aluminum alloy by Gerard (taken from ref. 19).
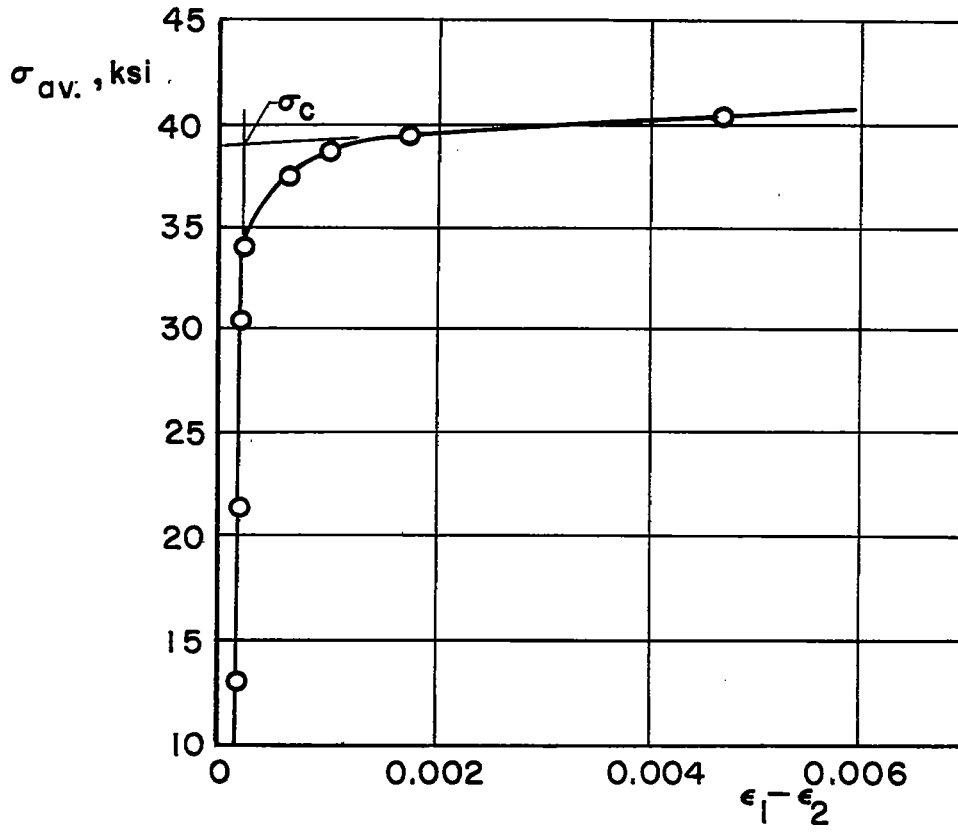
Figure 4.14.- Determination of critical load in Gerard's tests.
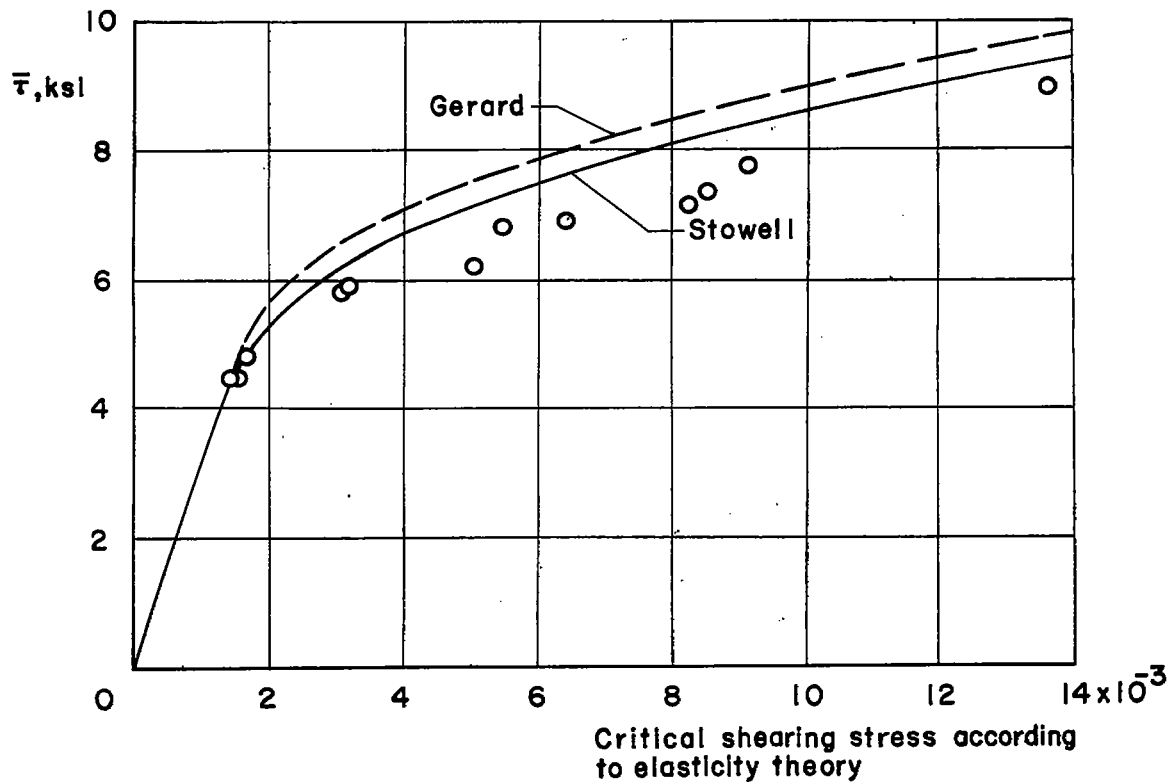
Figure 4.15.- Critical shearing stress $\tau_{\_}$ of an infinitely long plate
loaded in shear; theoretical curves for hinged and clamped edge
support. Tests with long sides clamped.
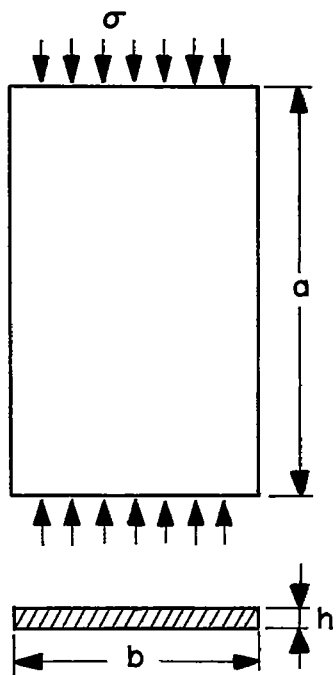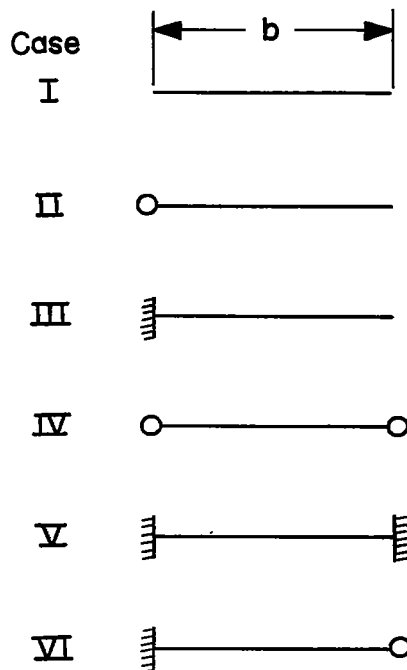
Figure 4.16.- Kollbrunner load cases on avional m alloys.

Test plate

Vertical supports

Base plate

Anchoring of the base plates

Plate under pressure
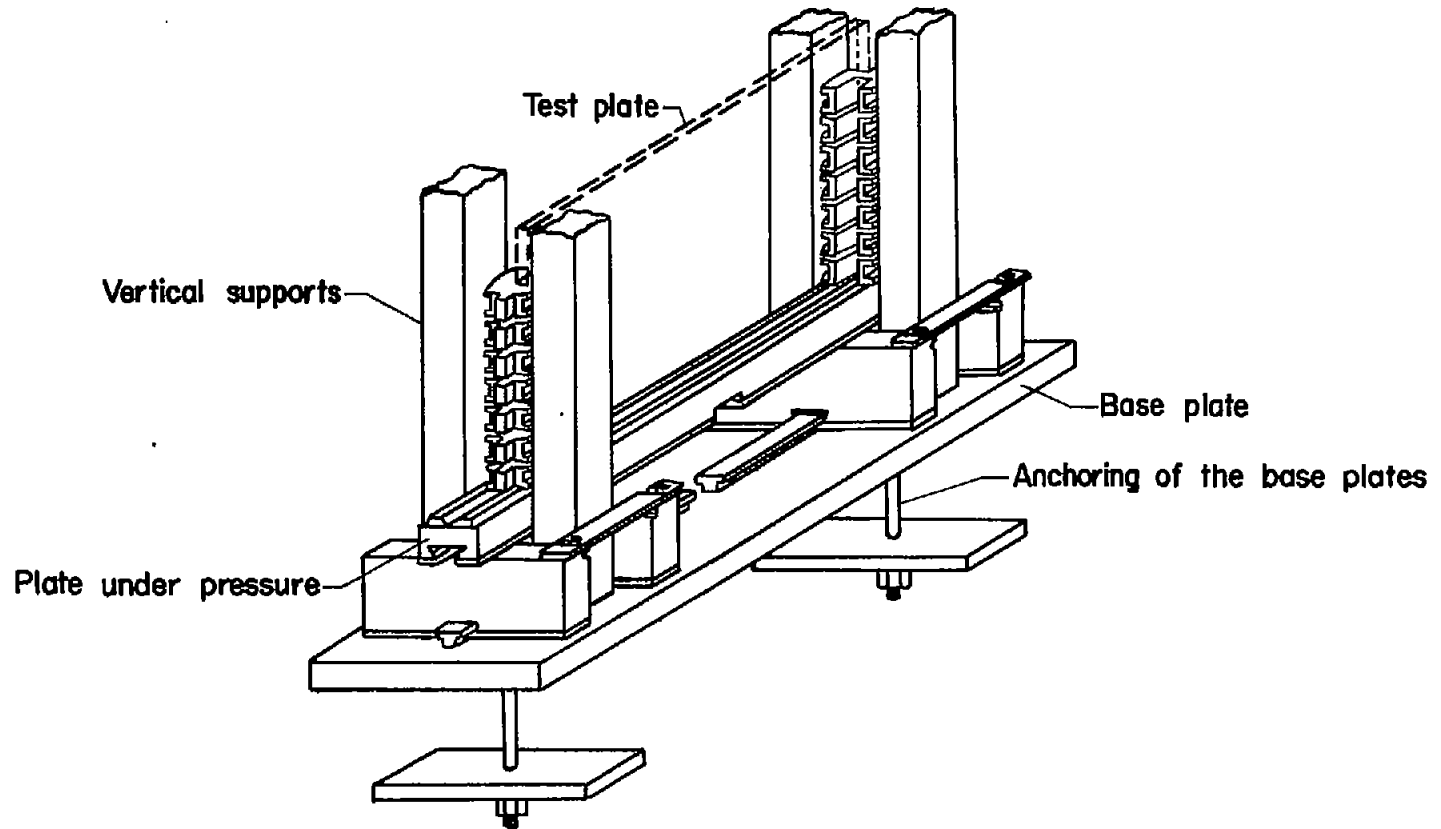
Figure 4.17.- Kollbrunner's experimental setup.

(a) Hinge type

(b) Fixed-clamping type
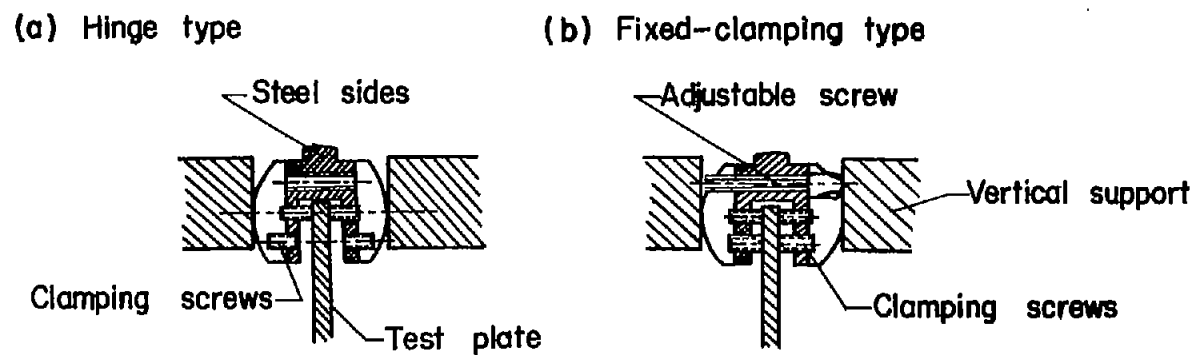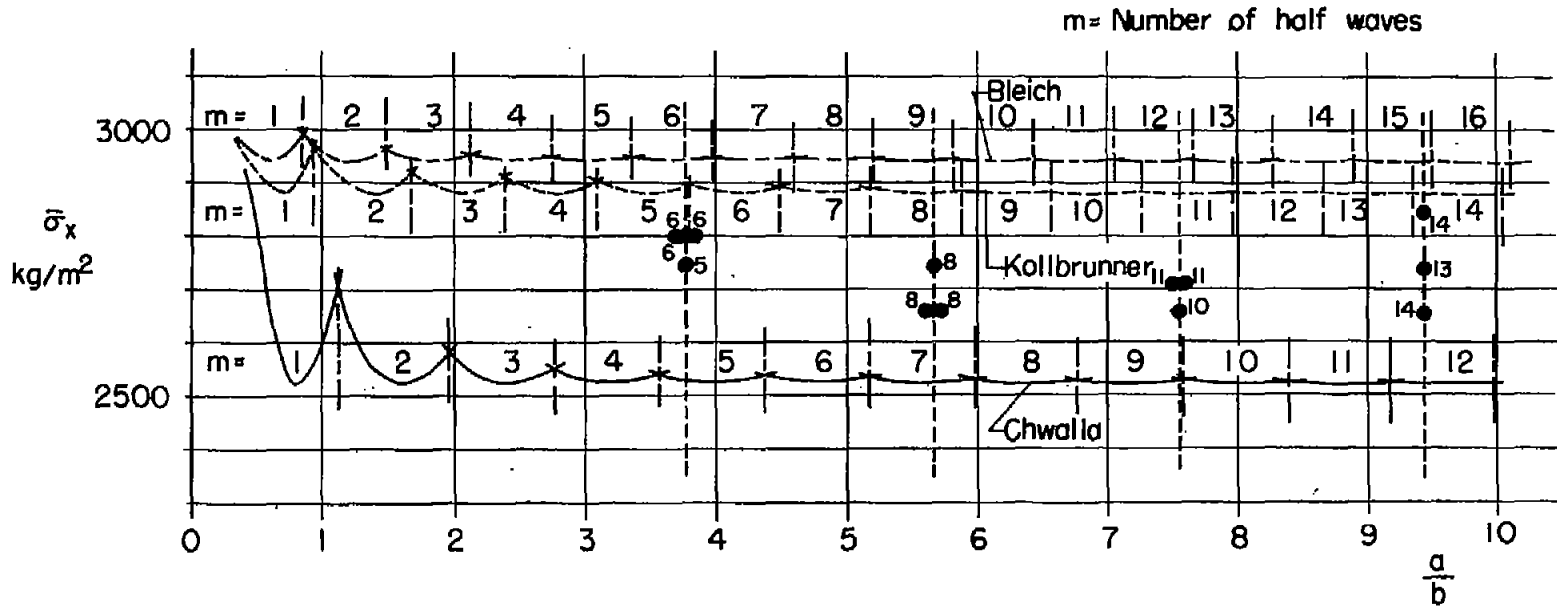

Figure 4.18.- Steel sides used by Kollbrunner.
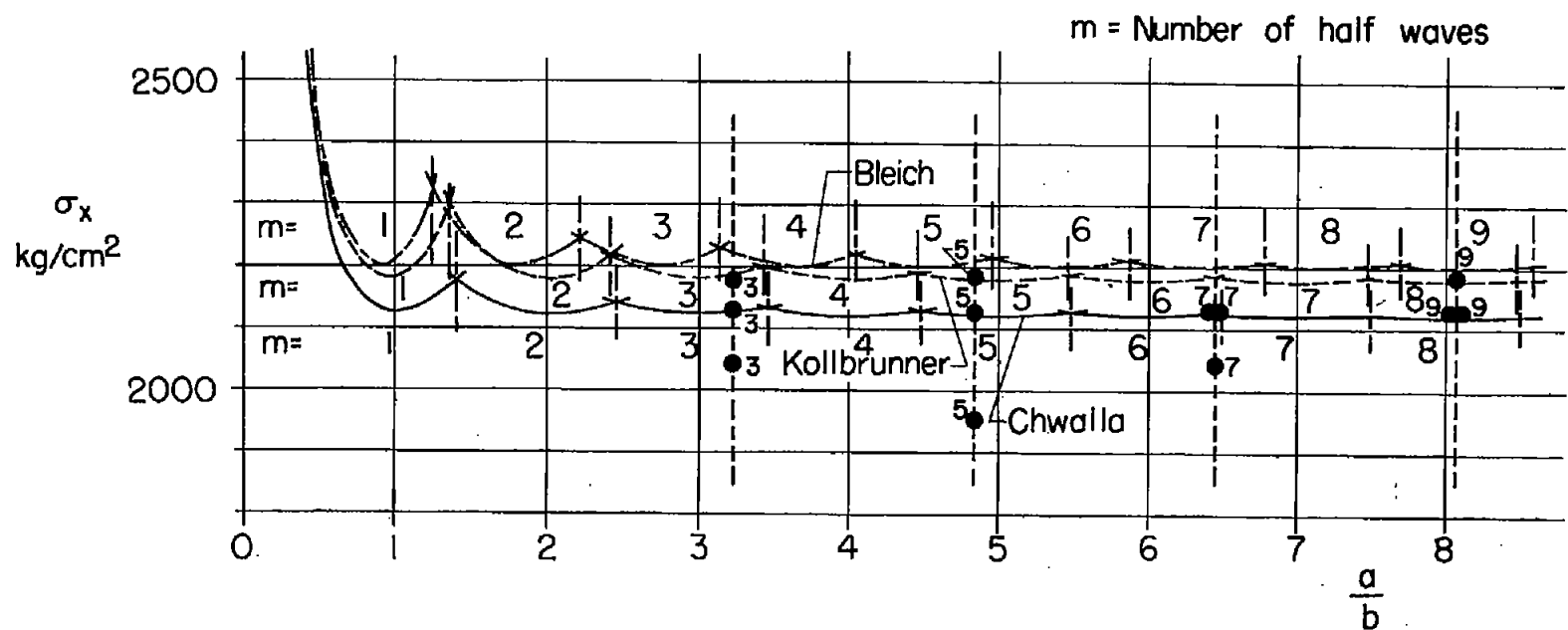
Figure 4.19.- Critical stress $\bar{\sigma}_x$ for load case IV of figure 4.16, b/h = 31 (from ref. 8).
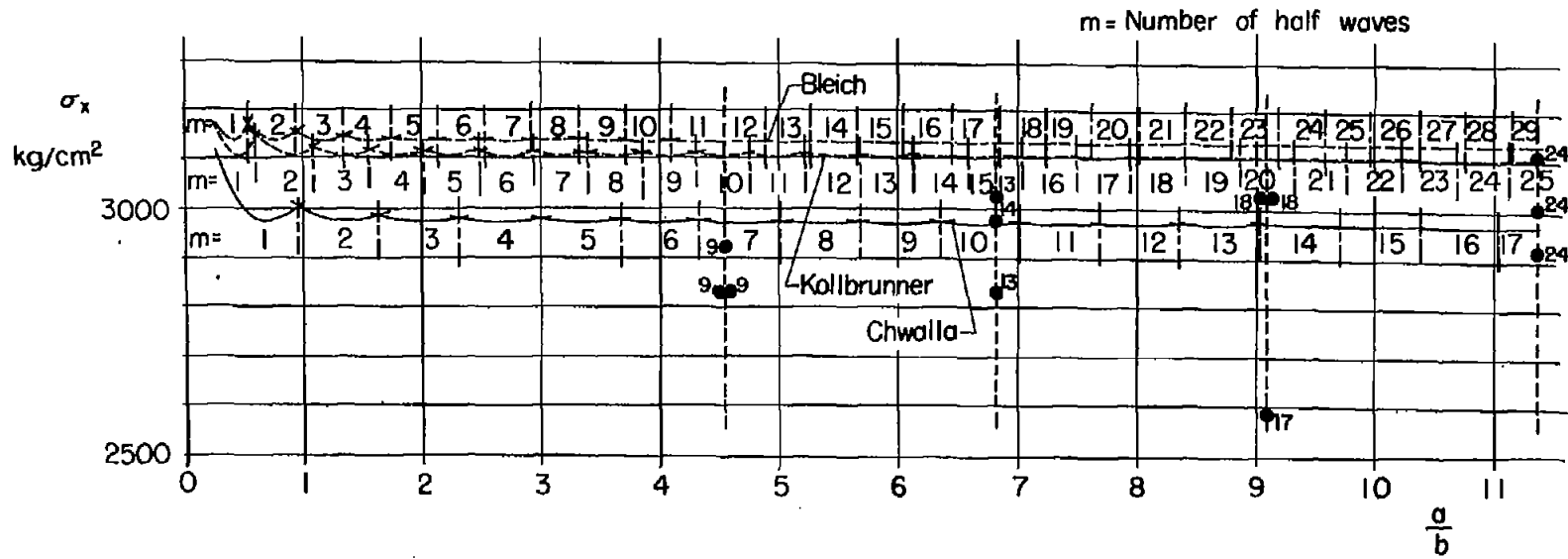
Figure 4.20.- Critical stress $\bar{\sigma}_x$ for load case V of figure 4.16,
b/h = 20 (from ref. 8).

Figure 4.21.- Critical stress $\bar{\sigma}_x$ for load case VI of figure 4.16,
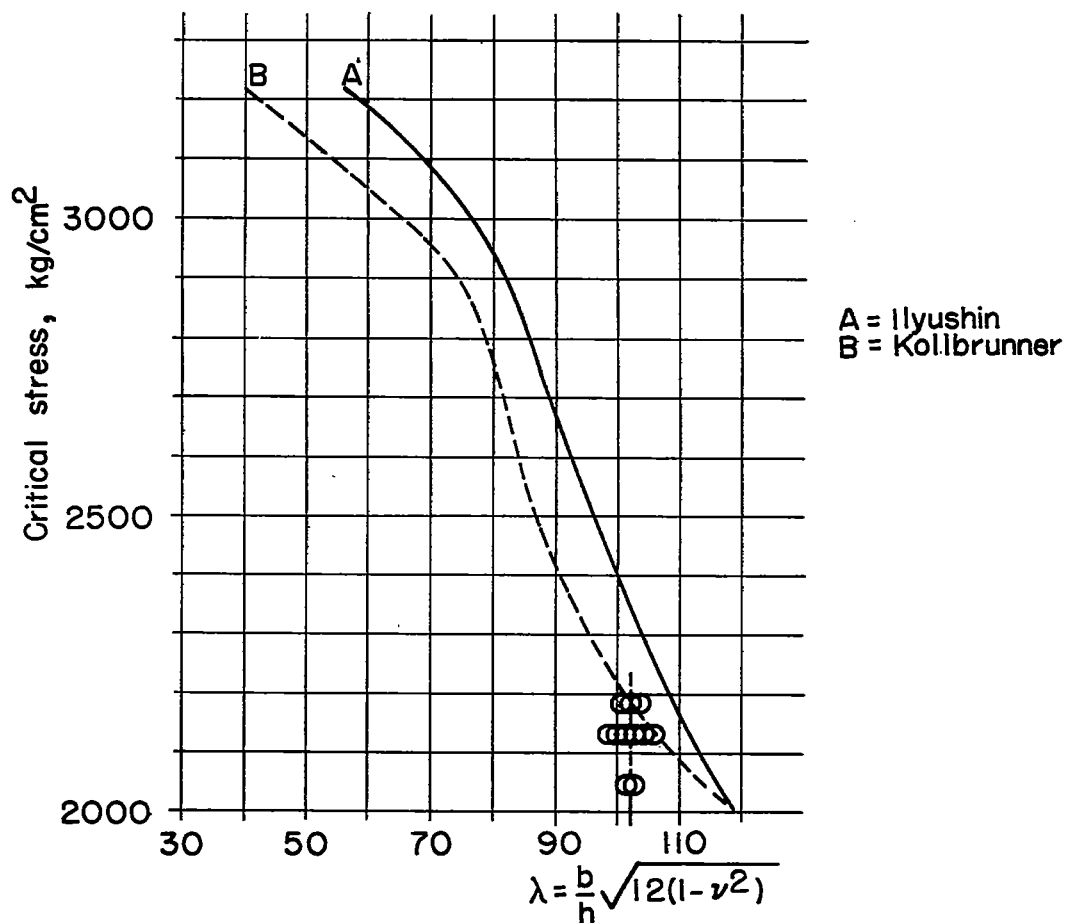b/h = 26.5 (from ref. 8).

Figure 4.22.- Critical stress $\bar{\sigma}_x$ for load case IV of figure 4.16 of infinitely long plate according to Kollbrunner and Ilyushin (taken from ref. 11).
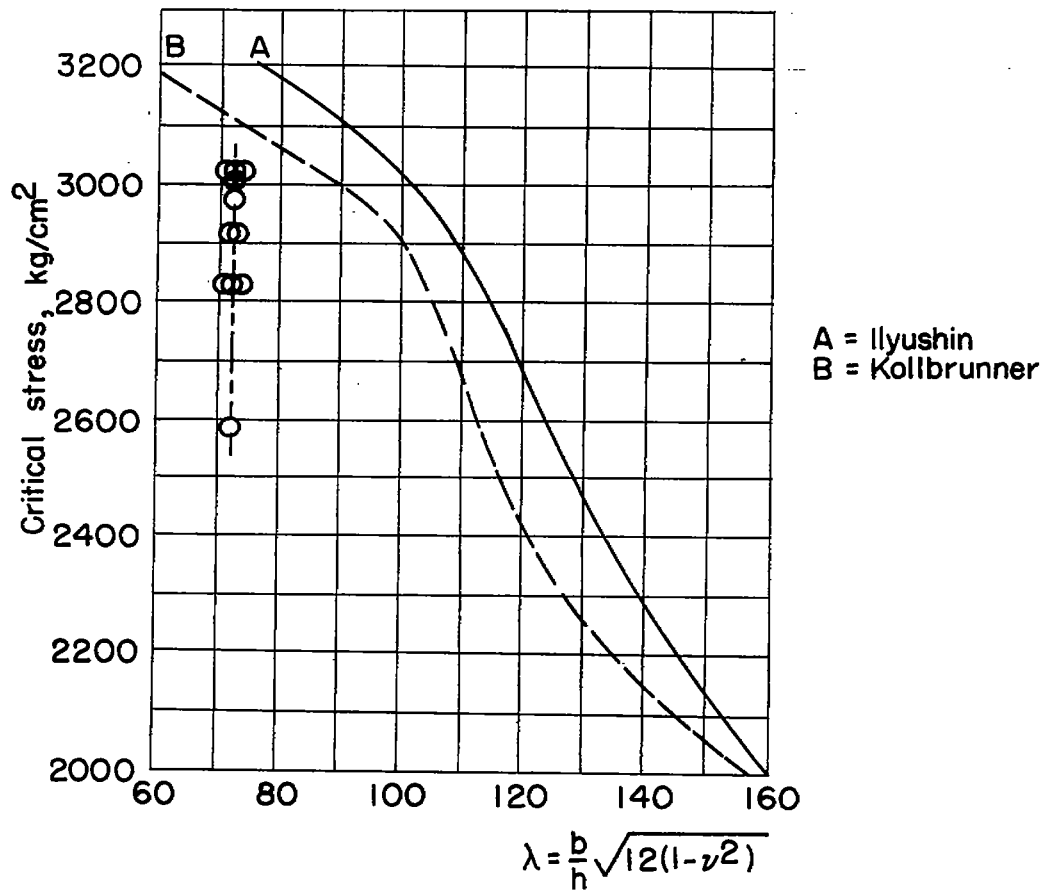
Figure 4.23.- Critical buckling stress for load case $\underline{V}$ of figure 4.16 on infinitely long plate according to Kollbrunner and Ilyushin.
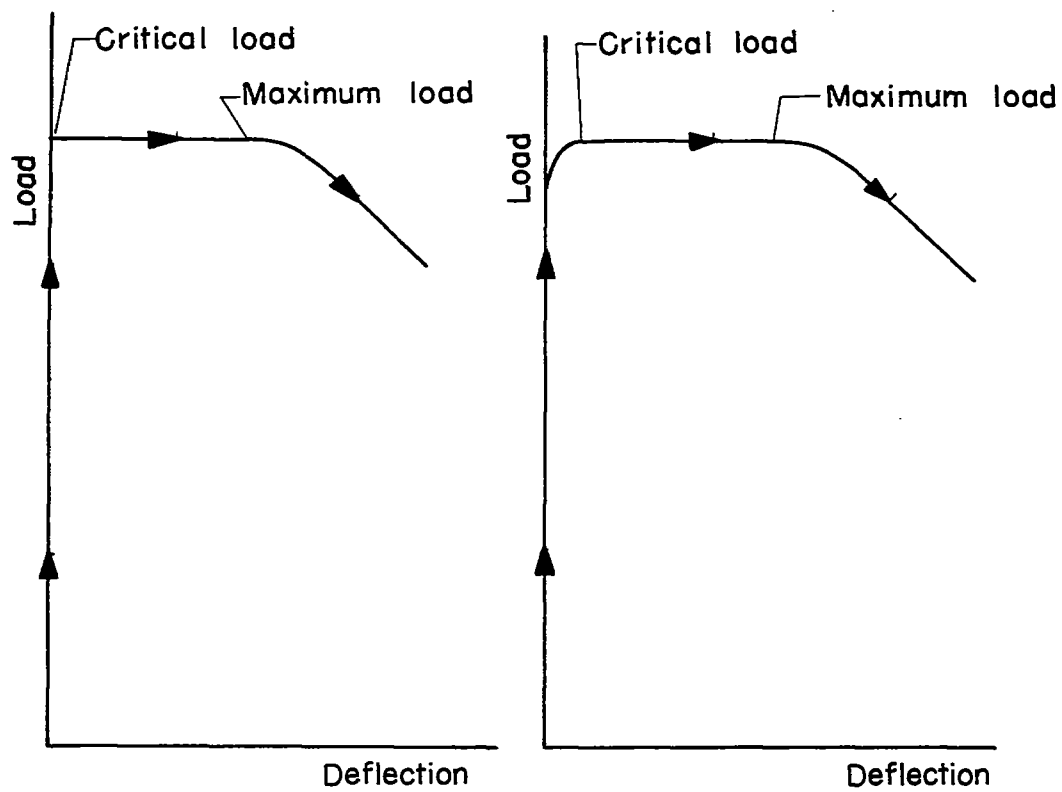
Figure 5.1.- Determination of critical load and maximum load in the
compression tests of reference 30. (Results of these tests given in
figs. 4.10 and 4.11.)